USE OF FIRE PLUME THEORY IN THE DESIGN AND ANALYSIS OF FIRE DETECTOR AND SPRINKLER RESPONSE

by
Robert P. Schifiliti

A Thesis

Submitted to the Faculty

of the

WORCESTER POLYTECHNIC INSTITUTE

in partial fulfillment of the requirements for the

Degree of Master of Science

in

Fire Protection Engineering

January 1986

APPROVED:

(Signed)

Prof. Richard L. Custer, Major Advisor

(Signed)

Dr. Craig L. Beyler, Associate Advisor

(Signed)

Prof. David A. Lucht, Head of Department

Notice of Disclaimer

This thesis references and uses correlations developed by Heskestad and Delichatsios for ceiling jet temperature and velocity from t^2 fires.

The correlations by Heskestad and Delichatsios were developed assuming that the test fuel had a heat of combustion of 20,900 kJ/kg and a convective heat release fraction of about 75%. Subsequently, experimentation showed that a heat of combustion equal to 12,500 kJ/kg would be a more accurate value for the wood cribs used in the test. Heskestad and Delichatsios subsequently published updated correlations based on this new value. Consequently, the correlations in this thesis are incorrect.

The correlations for t^2 fires were developed using data from a series of wood crib burn tests. The test fires had a convective heat release fraction of approximately 75%. Modeling fuels having different convective fractions will produce some degree of error.

In their updated paper, Heskestad and Delichatsios also provided correlations based only on the convective heat release rate. These correlations should be used when the convective fraction is significantly different than the 75% from the original test series.

The following references discuss these changes and their effects in more detail. They also discuss how correction factors can be applied to computer programs or models that use the older, incorrect correlations in order to adjust for the inherent error.

G. Heskestad and M. Delichatsios, "Update: The Initial Convective Flow in Fire", *Fire Safety Journal*, Volume 15, 1989, p. 471-475.

R.P. Schifiliti and W.E. Pucci, *Fire Detection Modeling: State of the Art, the Fire Detection Institute*, Bloomfield, CT, 1996.

NFPA 72, *National Fire Alarm Code*, National Fire Protection Association, Quincy, MA 1999.

- R.P. Schifiliti, March 31, 2000

ABSTRACT

This thesis demonstrates how the response of fire detection and automatic sprinkler systems can be designed or analyzed. The intended audience is engineers involved in the design and analysis of fire detection and suppression systems. The material presented may also be of interest to engineers and researchers involved in related fields.

National Bureau of Standards furniture calorimeter test data is compared to heat release rates predicted by a power-law fire growth model. A model for calculating fire gas temperatures and velocities along a ceiling, resulting from power-law fires is reviewed. Numerical and analytical solutions to the model are outlined and discussed.

Computer programs are included to design and analyze the response of detectors and sprinklers. A program is also included to generate tables which can be used for design and analysis, in lieu of a computer.

Examples show how fire protection engineers can use the techniques presented. The examples show how systems can be designed to meet specific goals. They also show how to analyze a system to determine if its response meets established goals. The examples demonstrate how detector response is sensitive to the detector's environment and physical characteristics.

ACKNOWLEDGEMENTS

I would like to thank Dick Custer, Jonathan Barnett and Craig Beyler for their help and advice which led to the conclusion of this thesis. I must also express my gratitude to Dr. Fitzgerald for his many years of guidance and to Wayne Moore for his continued support and friendship.

Most of all I thank my wife, Chris, for her love and understanding, without which I could not have completed this work.

TABLE OF CONTENTS

LIST OF TABLES

LIST OF ILLUSTRATIONS

NOMENCLATURE

a	alpha – fire intensity coefficient, BTU/sec^3 or kW/sec^2.
A	area, ft^2 or m^2.
A	$g/(C_pT_ar_0)$, ft^4/(sec^{2}BTU) or m^4/(sec^{2}kJ).
c	specific heat of detector element, BTU/(lbm°R) or kJ/(kg°K).
C_p	specific heat of air, BTU/(lbm°R) or kJ/(kg°K).
C	mass concentration of particles.
d	length over which D_u is measured, ft or m.
D	effective diameter of fuel bed, ft or m.
D	optical density, decibels (dB).
D	0.188 + 0.313r/H.
D_u	optical density per unit length, dB/ft or dB/m
Dt	delta t - change in time, seconds.
DT	delta T - increase above ambient in temperature of gas surrounding a detector, °F or °C.
DT_d	delta T_d - increase above ambient in temperature of a detector, °F or °C.
DT_p*	delta T_p* - change in reduced gas temperature.
f	functional relationship.
g	functional relationship.
g	gravitational constant, ft/sec^2 or m/sec^2.
h	convective heat transfer coefficient, BTU/(ft^{2}sec°F) or kW/(m^2°C).
H	ceiling height or height above fire, ft or m.
H_0	height above virtual origin of fire, ft or m.
H_c	heat of combustion, kJ/mole.

H_f heat of formation, kJ/mole.

I light intensity in the presence of smoke.

I_0 intensity of light under ambient conditions.

k absorption coefficient of smoke.

m mass, lbm or kg.

p positive exponent.

q_{cond} heat transferred by conduction, BTU/sec or kW.

q_{conv} heat transferred by convection, BTU/sec or kW.

q_{rad} heat transferred by radiation, BTU/sec or kW.

q_{total} total heat transfer, BTU/sec or kW.

Q heat release rate, BTU/sec or kW.

Q_P predicted heat release rate, BTU/sec or kW.

Q_T threshold heat release rate at response, BTU/sec or kW.

r radial distance from fire plume axis, ft or m.

R_e Reynolds number.

RTI response time index, $ft^{1/2}sec^{1/2}$ or $m^{1/2}sec^{1/2}$.

S spacing of detectors or sprinkler heads, ft or m.

t time, seconds.

t_c critical time - time at which fire would reach a heat release rate of 1000 BTU/sec (1055 kW), seconds.

t_r response time, seconds.

t_v virtual time of origin, seconds.

t_{2f} arrival time of heat front (for p = 2 power-law fire) at a point r/H, seconds.

t_{2f}* reduced arrival time of heat front (for p = 2 power-law fire) at point r/H, seconds.

t_p* reduced time.

T temperature, °F or °C.

T_a ambient temperature, °F or °C.

T_d detector temperature, °F or °C.

T_g temperature of fire gasses, °F or °C.

T_s rated operating temperature of a detector or sprinkler, °F or °C.

u instantaneous velocity of fire gases, ft/sec or m/sec.

u_o velocity at which Γ_0 was measured, ft/sec or m/sec.

u_p* reduced gas velocity.

v kinematic viscosity, ft^2/sec or m^2/sec.

$\underline{x}$ vectorial observation point, ft or m.

Y defined in equation

z_0 distance from top of combustible to virtual origin, ft or m.

Γ tau, detector time constant - mc/(hA), seconds.

Γ_0 tau measured at reference velocity u_0, seconds.

1. INTRODUCTION

The present practice in designing fire detection systems is to space heat detectors at intervals equal to a spacing listed by Underwriters Laboratories, Inc. Listed spacings are determined in full scale fire tests.

In the test, a burning pan of 190 proof denatured alcohol is located in the center of a test room. Sprinkler heads having a 160 degree Fahrenheit rated operating temperature are located on the ceiling in a square array having ten foot sides. The fire is in the center of the square. The distance between the fire and the ceiling is varied so that the 160 °F sprinkler head being used operates in approximately two minutes. Detectors of the type being tested are located at the corners of squares having 20, 30, 40 and 50 foot sides. See Figure 1. The spacing of the last detector to operate prior to a sprinkler head operating becomes the detector's listed spacing.

Smoke detectors do not have listed spacings. They are most often spaced according to manufacturers' recommendations. In most cases manufacturers recommend spacing smoke detectors thirty feet apart on smooth ceilings. This spacing is not based on any specific performance requirements but is simply a consensus that 30 foot spacing appears to provide adequate warning of a fire.

FIGURE 1

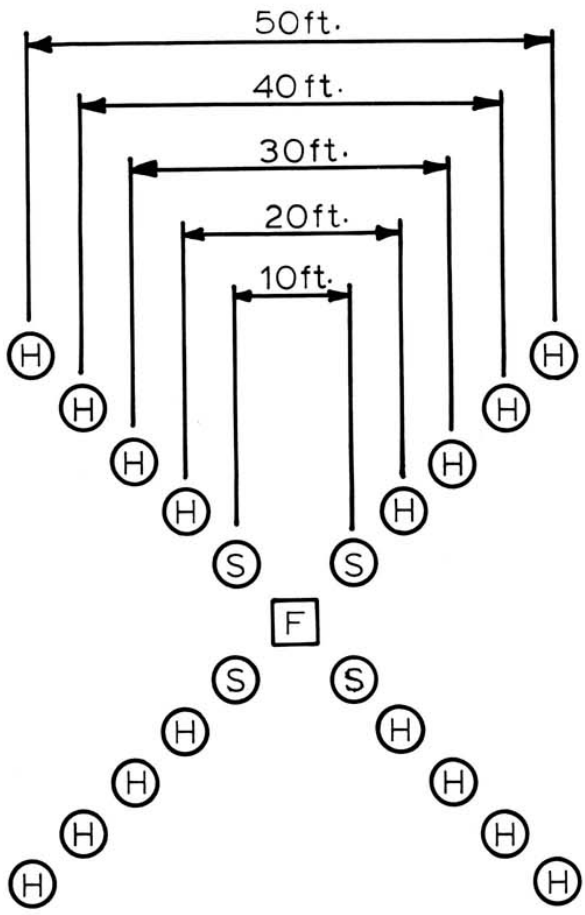

H HEAT DETECTOR
S SPRINKLER
F FIRE

DETECTOR TEST LAYOUT

In 1984 Appendix C was introduced into NFPA 72 E [1]. This appendix is a guide for designers and fire protection engineers to use in determining the spacing of detectors. Spacings recommended are a function of detector type and sensitivity, ceiling height, expected fire growth characteristics and the fire size to which the detector should respond.

Requirements for spacing and area of coverage for sprinkler heads are found in several codes and guides. These include NFPA 13, Standard for the Installation of Sprinkler Systems [2], Loss Prevention Data from Factory Mutual Engineering [3] and Recommended Practices from the Industrial Risk Insurers [4]. These requirements are based on a sprinkler system's ability to get water to the fire, stop its growth and possibly extinguish it. The requirements vary as a function of the degree of the hazard. They also allow for the ability of the water supply system to maintain a required flow and pressure at the sprinkler head.

Of all the codes and guides, only NFPA 72 E, Appendix C, allows the designer to engineer the response of a fire detection or sprinkler system. Sprinkler heads are included in this discussion since they are heat responsive devices. For the purposes of this paper, the terms sprinkler head and heat detector can be interchanged.

To design a system using Appendix C, the designer must

know certain design parameters and system goals. These include ceiling height and ambient temperature. It is also necessary to know the sensitivity and the threshold alarm level of the detector to be used as well as the expected fire growth rate. The system's goals for property protection, business interruption protection and life safety must be redefined in terms of a threshold heat release rate at which detection must occur. The ability to change any of these variables gives engineers a chance to design systems with a broad range of goals and materials.

Appendix C is based on a report issued by the Fire Detection Institute in 1979 titled "An Analysis of The Report on Environments of Fire Detectors" [5]. The report analyses the results of the first phase of a research program. The research was conducted by Factory Mutual Research Corporation (FMRC) and coordinated by the National Bureau of Standards (NBS) for the Fire Detection Institute. Gunner Heskestad and Michael Delichatsios wrote the original report for FMRC and NDS [6]. Collecting data on variables that effect the response of a fire detector was the main objective of the research program titled "Environments of Fire Detectors".

The majority of fire research has been involved with open flaming combustion. Not enough research has been done on smoldering combustion to allow definitive models of smoldering to be developed.

This thesis examined the flaming fire growth model which Heskestad and Delichatsios used in their work. The model was compared to data from fire tests at the National Bureau of Standards, Center for Fire Research. Sprinkler, heat detector and smoke detector response models are also discussed.

An analytic solution to the equations proposed by Heskestad and Delichatsios was found by Beyler [7]. A computer program was written to solve the equations and allow the response of detection and sprinkler systems to be designed. A technique was developed to solve the equations backwards which is useful in analyzing the response of existing systems. This algorithm has been included in the computer program.

Tables which can be used instead of the computer program were generated using a second computer program. The tables are tools which engineers can use when designing new or analyzing existing fire detection or sprinkler systems.

Examples were worked using both the program and the tables. The examples show the sensitivity of the response model to the variables which the engineer selects. While this paper is meant to show how one fire plume model can be used to design or analyze the response of detectors and sprinklers, the techniques presented apply to other models as well.

2. REVIEW OF FIRE PLUME RESEARCH

Fire tests done by Factory Mutual Research Corporation for the Fire Detection Institute were conducted between August 1975 and April 1976 [6]. Eighteen tests were conducted at FM's West Glocester, Road Island facility. Thirty one tests were conducted at their Norwood, Massachusetts test center.

Tests done at the West Glocester facility were designed to measure the effects of ceiling height and fire growth rate on the response of fire detectors. These tests included only open flaming fires and no smoldering fires. All tests were conducted under a large, flat ceiling with no walls.

Three ceiling heights were selected for the tests. They were, 8 ft, 15 ft, and 29 ft. The height of the ceiling above the fuel surface changed with each different fuel configuration. Fire growth rate was varied by using three different wood crib configurations. This gives nine possible combinations of fire growth rate and ceiling height. Several of the tests were repeated to help determine the repeatability of the testing procedures.

The thirty one tests conducted at the Norwood test center were designed to measure the effects of the material burning on the response of fire detectors. In twenty of the tests the combustion mode was open flaming. Eleven tests

were conducted to measure the effects of smoldering combustion. Materials for the Norwood tests were wood cribs, cotton fabric, blocks of foamed polyurethane and wire with polyvinyl chloride insulation [6].

Temperature, gas velocity and optical density were measured at various locations along the ceiling. Cumulative weight loss of the fuel was also measured. In addition several commercially available smoke and heat detectors were grouped together and located at several positions along the test ceiling. The response of these detectors was recorded. These data are summarized in the Phase 1, Volume 1 report by Heskestad and Delichatsios [6].

A set of functional relationships for the temperature and velocity of ceiling jet gases has been proposed by Heskestad [8] [9]. The expressions relate fire size, fire growth rate, height above the fire, radial distance from the fire, gas temperature and gas velocity for the general class of fires called power-law fires. In power-law fires the instantaneous heat release rate varies according to:

$$Q = at^p \qquad [1]$$

where a is alpha, a fire growth coefficient, t is time and p is a positive exponent. The functional relationships proposed by Heskestad are:

$$u/[a^{1/(3+p)}H^{(p-1)/(3+p)}] = f\{t/[a^{-1/(3+p)}H^{4/(3+p)}], \underline{x}/H\}$$

$$DT/[a^{2/(3+p)}H^{-(5-p)/(3+p)}] = g\{t/[a^{-1/(3+p)}H^{4/(3+p)}], \underline{x}/H\}$$

Here u is the instantaneous velocity of the gas, H is the height of the ceiling above the fire, $\underline{x}$ is the observation point measured perpendicular to the fire plume axis and DT is delta T, the rise in gas temperature. The terms containing u, DT and t are referred to as reduced velocity (u_p*), reduced temperature rise (DT_p*) and reduced time (t_p*) respectively.

For most ceiling jet models it is necessary to know the height of the ceiling above the focal point of the fire plume. The focal point is also called the origin or virtual origin of the plume. See Figure 2. For steady fires it has been shown [10] that the location of the origin can be predicted by:

$$z_0(ft) = -1.02\ D(ft) + 0.083\ Q(BTU/sec)^{2/5} \qquad [2]$$

Where D is the effective diameter of the fuel and Q is the total heat release rate. This relationship may not be accurate for fires where a great deal of the combustion is taking place in the fuel itself and not primarily above the surface. Fuel arrays with good ventilation such as open wood cribs, might not behave according to the equation. A fire in

FIGURE 2

FIRE PLUME

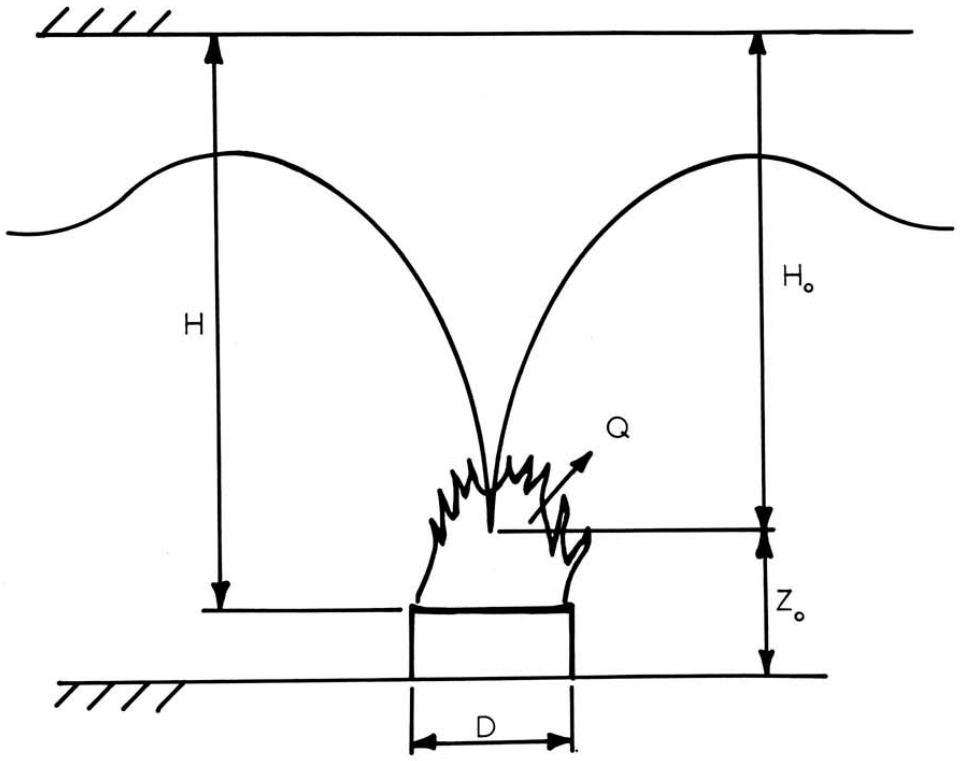

a well ventilated wood crib will have a substantial amount of combustion taking place inside the crib, below the surface.

Heskestad and Delichatsios [6] chose to use the height above the fuel surface H, in their work. Later, the effects of this assumption will be tested by comparing results obtained using the height above the fuel surface, H, to results using the height above the virtual origin, H_0.

In analyzing test data it was found that many fires closely follow the power-law growth model with p = 2 [6]. The functional relationships then take the form:

$$u_2^* = f\ (t_2^*,\ r/H)$$

$$DT_2^* = g\ (t_2^*,\ r/H)$$

Here r is the radial distance from the fire.

For convenience Heskestad and Delichatsios define the critical time, t_c, by the following relationship:

$$a = 1000\ (BTU/sec)\ /\ [t_c(sec)]^2 \qquad [3]$$

or:

$$t_c = [1000\ (BTU/sec)\ /\ a]^{1/2} \qquad [4]$$

The critical time is the time at which the fire would reach a

heat output of 1000 BTU/sec. Heskestad and Delichatsios used t_c (in lieu of a) to describe the rate of fire growth in the formulas they present. The word critical may be misleading as t_c does not represent any particularly important event in the growth of a fire. t_c is merely used for convenience in place of alpha.

Heskestad and Delichatsios found the following relationships to agree closely with data collected in the test series [6]

$$t = (0.251\ t_c^{2/5} H^{4/5})\ t_2^* \qquad [5]$$

$$DT = (15.8\ t_c^{-4/5} H^{-3/5})\ DT_2^* \qquad [6]$$

$$u = (3.98\ t_c^{-2/5} H^{1/5})\ u_2^* \qquad [7]$$

and:

$$t_{2f}^* = 0.75 + 0.78(r/H) \qquad [8]$$

If $t_2^* \leq t_{2f}^*$ then: $DT_2^* = 0$

Else:

If $t_2^* > t_{2f}^*$ then:

$$t_2^* = 0.75 + 2.22(DT_2^*/1000)^{0.781} + [0.78 + 3.69(DT_2^*/1000)^{0.870}](r/H) \qquad [9]$$

$$u_2^*/(DT_2^{*1/4}) = 0.36(r/H)^{-0.315} \qquad [10]$$

Here t_{2f}* is the reduced arrival time of the heat front at the detector location. Equation 8 is used with Equation 5 to calculate the actual time when the heat front reaches the detector.

By rearranging the terms, Equation 9 is expressed in terms of t_{2f}*

$$t_2^* = t_{2f}^* + 2.22(DT_2^*/1000)^{0.781} + 3.69(DT_2^*/1000)^{0.870}(r/H) \quad [11]$$

The data show these relationships cease to be valid at temperatures of about 1600 degrees F along the axis of the fire plume [6]. The equations assume open flaming combustion is established and the fire obeys the power-law growth model with p = 2.

The equations do not model smoldering combustion. This is because during smoldering, most of the heat being released by the combustion process is being absorbed by the fuel itself. This heat liberates additional volatiles from the fuel. These equations are used only when sufficient volatiles are being driven from the fuel and are reacting in a combustion zone above the fuel surface. In addition, a sufficient amount of the heat being released in the combustion zone must be carried away from the fuel in a rising convective plume.

When any fluid flows across a flat plate such as a ceiling, the velocity of the fluid immediately adjacent to the plate is zero. Moving away from the ceiling the flow increases to full flow. This is shown graphically in Figure 3. Within the small boundary layer, the effects of ceiling drag and heat transfer to the ceiling can not be neglected. The thickness of this boundary layer is a function of the velocity and the kinematic viscosity of the fire gases.

Detectors, thermocouples and velocity probes used in the tests at Factory Mutual were located four and one half to five inches below the ceiling. Based on model calculations, Beyler [7] concludes that these measurements were taken outside of the viscous boundary layer, which he estimated to be a maximum of three inches in the tests. Hence the similarity equations proposed by Heskestad are used to model the flow and temperature of fire gases outside of the boundary layer.

The value of these relationships is that they can be used to calculate the gas temperature and velocity in the vicinity of the ceiling at some distance r, from the fire. These calculations are at time t, for a fire with a growth characteristic alpha, or a critical time t_c and at some position r and H. In this form the equations are solved numerically for the fire gas temperature and velocity.

FIGURE 3
VISCOUS AND THERMAL
BOUNDARY LAYERS

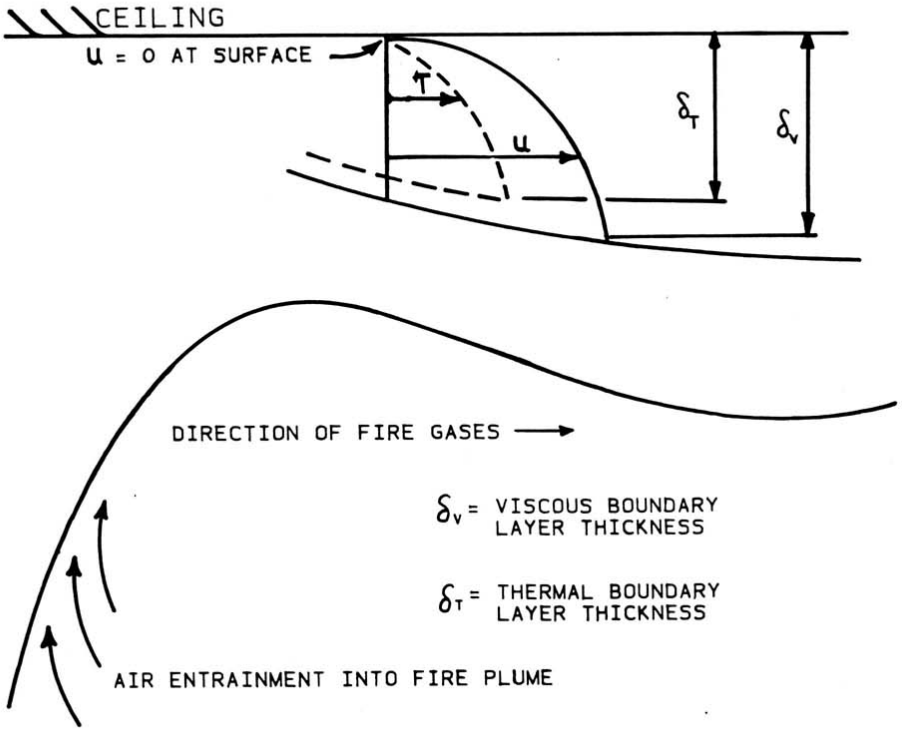

AT SURFACE, TEMPERATURE OF GAS = TEMPERATURE OF CEILING

As part of their tests at Factory Mutual Heskestad and Delichatsios [6] monitored the optical density per unit length D_u, at various locations along the ceiling. This is done by measuring the intensity of a light beam falling on a photo cell before the presence of smoke I_0, and during the presence of smoke I. The definition of optical density is:

$$D = -10 \log_{10}(I/I_0) \text{ dB} \qquad [12]$$

This is customarily expressed in terms of the length, d (meters or feet), over which the attenuation of the light beam was measured:

$$D_u = D/d \quad (\text{dBm}^{-1} \text{ or } \text{dBft}^{-1}) \qquad [13]$$

The transport of smoke from a fire is driven primarily by buoyant flows generated by the fire. Smoke movement is also affected by ambient temperatures and air movements as well as fans and air handling equipment in buildings. Discussion here is limited to smoke transport caused directly by the fire.

The relationship between optical density and the mass concentration of particles in the atmosphere C, is given by the Beer-Lambert law:

$$I = I_0 \exp(-kdC) \qquad [14]$$

where k is the absorption coefficient of the smoke. It has been shown [11] that k is dependent on the particle size distribution of the smoke. However, if it is assumed that particle size distribution does not vary appreciably as the smoke is transported away from the fire, the optical density is directly proportional to the mass concentration of particles in the atmosphere [6].

When certain assumptions are met, it has be shown that the mass concentration of particles at a particular position and time is a function of the change in temperature [6].

$$C = f(DT)$$

The most important assumptions are that there is no heat transfer between the fire gases and the ceiling and that the production of smoke is proportional to the mass burning rate. It must also be assumed that the products of combustion do not continue to react once they leave the initial combustion zone.

In analyzing the test data, Heskestad and Delichatsios looked for a relationship between D_u and the change in temperature along the ceiling. They plotted the ratio D_u/DT as a function of time for several of the test fires. The ratios were plotted for several different locations along the ceiling.

The graphs show that the ratio varies with time for a given combustible. For wood crib fires D_u/DT varied from 0.015 to 0.055 $°F^{-1}$ ft^{-1}. The largest variation was for burning PVC insulation which ranged from 0.1 to 1.0 $°F^{-1}$ ft^{-1}. Several tests showed the affects of heat loss to the ceiling. In these tests, the ratio D_u/DT was greater at radial positions farther from the fire. Despite this variation Heskestad and Delichatsios concluded that D_u/DT could be treated as a constant for a given combustible at a height H and a distance r from the fire. They also concluded that heat transfer to the ceiling becomes important at r/H ratios greater than 4. Table 1 gives representative values of D_u/DT for certain fuels. This table is reproduced from Reference 6. The fact that D_u/DT did vary, shows that additional research is needed to define a model for the production and transport of smoke in a fire.

The functional relationships proposed by Heskestad and Delichatsios assume the fire grows as a p = 2 power-law fire. It is important then to determine if this fire growth model is valid for fires involving common combustibles. To test the model, the instantaneous heat release rate predicted by:

$$Q = at^2 \qquad [15]$$

must be compared to heat release rates measured in independent tests of furnishings and other fuels.

TABLE 1

Representative Values of D_u/DT

for Flaming and Spreading Fires

(Reproduced from Reference 6)

	Material	$10^2 D_u/DT$ (ft^{-1} $°F^{-1}$)
1.	Wood (Sugar Pine, 5% Moist. Content)	0.02
2.	Cotton Fabric (Unbleached Muslin)	0.01/0.02
3.	Paper Wastebasket	0.03
4.	Polyurethane Foam	0.4
5.	Polyester Fiber (in Bed Pillow)	0.3
6.	PVC Insulation on Hook-up Wire	0.5/1.0
7.	Foam Rubber/Polyurethane in Sofa Cushion	1.3

See Reference 6 for a more complete description of the materials and for references to the test data.

3. NATIONAL BUREAU OF STANDARDS FURNITURE CALORIMETER TESTS

A large scale calorimeter for measuring heat release rates of burning furniture has been developed at the National Bureau of Standards [12]. The furniture calorimeter was developed to obtain a data base of heat release rates to help researchers develop accurate, small scale tests.

The calorimeter measures the burning rate of specimen under open air conditions. In an actual room, the burning rate is affected by walls or other objects close to the burning item. It is also affected by radiation from hot gases collecting at the ceiling and by the availability of fresh air for combustion. These factors can increase or decrease the heat release rate at any point in time.

In the furniture calorimeter, heat release rate data are obtained by measuring the amount of oxygen consumed during the fuel's combustion. This technique is based on the heat release per unit of oxygen consumed being near constant for most common combustibles [13] [14]. A table of $H_{c,ox}$ for selected fuels is compiled in Drysdale's "An Introduction to Fire Dynamics" [15].

The heats of combustion of fuels vary widely. Nevertheless when expressed in terms of oxygen consumption, they are found to lie in narrow limits. Huggett [13] found $H_{c,ox}$ = -12.72 kJ/g plus or minus three percent for typical

organic liquids and gases. He also found that polymers have $H_{c,ox}$ = -13.02 kJ/g plus or minus four percent.

Multiplying $H_{c,ox}$ by the rate of oxygen consumption gives the heat release rate. Thus the heat release rate of a fire can be determined by measuring the rate of oxygen use during the combustion process.

In the NBS furniture calorimeter the amount of oxygen consumed during combustion is found by measuring the amount of oxygen in the exhaust stream which is collected in a large hood. The difference between the amount of oxygen measured in the combustion products and that found in ambient air is the amount used in the combustion process. Corrections are made for the presence of carbon dioxide and carbon monoxide in the products of combustion.

The furniture calorimeter was tested and calibrated using a metered natural gas burner. Heat release rates determined from the rate of gas consumption were compared to the heat release rates determined from oxygen depletion theory. The apparatus was tested at heat release rates between 138 and 1343 kW (supplied to the burner). The results calculated by oxygen depletion theory varied from 125 to 1314 kW. Errors were found to be between 2 and 10 percent [12].

The National Bureau of Standards conducted tests in the furniture calorimeter to study the characteristics of several classes of furnishings. Two published reports, References 11 and 15, describe the tests and the data collected. The data include heat release rates, target irradiance, mass loss and particulate conversion (based on smoke production and mass loss).

Furniture calorimeter tests are free burn or open air tests. The tests conducted by Heskestad and Delichatsios [6] were also open air tests since they were conducted under a large flat ceiling with no walls. Data from the NBS tests can be used to test the generality of the fire growth model which Heskestad and Delichatsios used in their fire detector response model.

4. COMPARISON OF CALORIMETER TEST DATA WITH THE POWER-LAW FIRE GROWTH MODEL

The equations proposed by Heskestad and Delichatsios to predict the temperature and velocity of a fires combustion products at a point along the ceiling are dependent on the assumption that the fire grows according to:

$$Q = at^2 \qquad [16]$$

or:

$$Q\ (kW) = [1050 / t_c^2]\ t^2 \qquad [17]$$

The task here is to determine if this p = 2, power-law fire growth model is accurate for use in developing a fire detector response model. Is this model useful for predicting the heat release rate of common fuels?

This type of fire growth model predicts the heat release rate of a single item burning. Multiple items involved in a fire might follow this type of power-law growth. However the ability to predict what combination of items in a room will be burning and the effects each has on the other is beyond the scope of this investigation. In addition, when designing fire detection or sprinkler systems the goal is usually to have the system respond before a second item becomes involved.

To test the power-law fire growth model, heat release

rate data were obtained for forty tests conducted in the furniture calorimeter at the National Bureau of Standards. The results of these tests are contained in two NBS publications, References 12 and 16. W.D. Walton, one of the NBS researchers, made the data available on a diskette which can be read by an IBM PC.

The test data is for furnishings such as upholstered chairs, loveseats, sofas, wood and metal wardrobe units, bookcases, mattresses and boxsprings. Table 2 is a summary description of these tests. This table includes the test numbers used by the original researchers in their reports [12] [16].

For each of the tests, the data were loaded into a spreadsheet program created using LOTUS 1-2-3, a spreadsheet, database and graphics software package developed by LOTUS Development Corporation in Cambridge Massachusetts. The spreadsheet facilitated formatting and plotting of the data.

If the data follows a power-law model, a log-log graph of heat release rate versus time should plot as a straight line. The slope of the straight line is the exponent p in the power-law equation. The y intercept is alpha, the fire intensity coefficient.

Data from six of the NBS tests were plotted. A regression of heat release upon time was done to produce an

TABLE 2

SUMMARY OF NBS CALORIMETER TESTS

FIG. NO.	TEST NO.		DESCRIPTION
Al	TEST	15	METAL WARDROBE 41.4 KG (TOTAL)
A2	TEST	18	CHAIR F33 (TRIAL LOVESEAT) 39.2 KG
A3	TEST	19	CHAIR F21 28.15 KG INITIAL STAGE OF FIRE GROWTH
A4	TEST	19	CHAIR F21 28.15 KG LATER STAGE OF FIRE GROWTH
A5	TEST	21	METAL WARDROBE 40.8 KG (TOTAL) AVERAGE GROWTH
A6	TEST	21	METAL WARDROBE 40.6 KG (TOTAL) LATER GROWTH
A7	TEST	21	METAL WARDROBE 40.8 KG (TOTAL) INITIAL GROWTH
AS	TEST	22	CHAIR F24 28.3 KG
A9	TEST	23	CHAIR F23 31.2 KG
A10	TEST	24	CHAIR F22 31.9 KG
All	TEST	25	CHAIR F26 19.2 KG
A12	TEST	26	CHAIR F27 29.0 KG
A13	TEST	27	CHAIR F29 14.0 KG
A14	TEST	28	CHAIR F28 29.2 KG
A15	TEST	29	CHAIR F25 27.8 KG LATER STAGE OF FIRE GROWTH
A16	TEST	29	CHAIR F25 27.8 KG INITIAL STAGE OF FIRE GROWTH
A17	TEST	30	CHAIR F30 25.2 KG
A18	TEST	31	CHAIR F31 (LOVESEAT) 39.6 KG
A19	TEST	37	CHAIR F31 (LOVESEAT) 40.40 KG
A20	TEST	38	CHAIR F32 (SOFA) 51.5 KG
A21	TEST	39	1/2 IN. PLYWOOD WARDROBE WITH FABRICS 68.5 KG
A22	TEST	40	1/2 IN. PLYWOOD WARDROBE WITH FABRICS 68.32 KG
A23	TEST	41	1/8 IN. PLYWOOD WARDROBE WITH FABRICS 36.0 KG
A24	TEST	42	1/8 IN. PLY.WARD. W/FIRE-RET. INT. FIN. INITIAL
A25	TEST	42	1/8 IN. PLY.WARD. W/FIRE-RET. INT. FIN. LATER
A26	TEST	43	REPEAT OF 1/2 IN. PLYWOOD WARDROBE 67.62 KG.
A27	TEST	44	1/8 IN. PLY. WARDROBE W/F-R. LATEX PAINT 37.26KG
A28	TEST	45	CHAIR F21 28.34 KG (LARGE HOOD)
A29	TEST	46	CHAIR F21 28.34 KG
A30	TEST	47	CHAIR ADJ. BACK METAL FRAME, FOAM CUSH. 20.8 KG
A31	TEST	48	EASY CHAIR C07 (11.52 KG)
A32	TEST	49	EASY CHAIR 15.68KG (F-34)
A33	TEST	50	CHAIR METAL FRAME MINIMUM CUSHION 16.52 KG
A34	TEST	51	CHAIR MOLDED FIBERGLASS NO CUSHION 5.28 KG
A35	TEST	52	MOLDED PLASTIC PATIENT CHAIR 11.26 KS
A36	TEST	53	CHAIR METAL FRAME W/PADDED SEAT AND BACK 15.5 KG
A37	TEST	54	LOVESEAT METAL FRAME WITH FOAM CUSHIONS 27.26 KG
A38	TEST	55	GROUP CHAIR METAL FRAME AND FOAM CUSHION 6.08 KG
A39	TEST	56	CHAIR WOOD FRAME AND LATEX FOAM CUSHIONS 11.2 KG
A40	TEST	57	LOVESEAT WOOD FRAME AND FOAM CUSHIONS 54.60 KG
A41	TEST	61	WARDROBE 3/4 IN. PARTICLEBOARD 120.33 KG
A42	TEST	62	BOOKCASE PLYWOOD WITH ALUMINUM FRAME 30.39 KG
A43	TEST	64	EASYCHAIR MOLDED FLEXIBLE URETHANE FRAME 15.98KG
A44	TEST	66	EASY CHAIR 23.02 KG
A45	TEST	67	MATTRESS & BOXSPRING 62.36 KG, LATER FIRE GROWTH
A46	TEST	67	MATTRESS & BOX. 62.36 KG, INITIAL FIRE GROWTH

equation for the best fit line to the data. A statistical least squares method was used to establish the equation for the straight line.

Figure 4 is a log-log plot of data from Test 22 for t = 0 to t = 660 seconds, which is when the peak heat release rate was reached during the test. Superimposed on the data is the best fit line which was calculated using the data from t = 0 to the peak heat release rate. This regression results in an alpha of 0.0241 kW/sec^2 and an exponent, p, equal to 1.3762.

The best fit line does not appear to be a good model for this data. However, a closer look shows that the data appear to fall along a straight line from about t = 400 seconds to the peak. Figure 5 shows a best fit line which was found by doing a statistical regression on the data from 400 to 660 seconds. This line is a much better model of the data. Alpha was calculated to be 8×10^{-11} and p was found to be 4.56.

In this case, 400 seconds was arbitrarily selected as the starting point for the regression analysis. This point will be referred to as the virtual time of origin, t_v, the time when the fire begins to follow a power-law model. The virtual origin could be defined as the time at which the fire reaches some minimum heat release rate or the time at

FIGURE 4

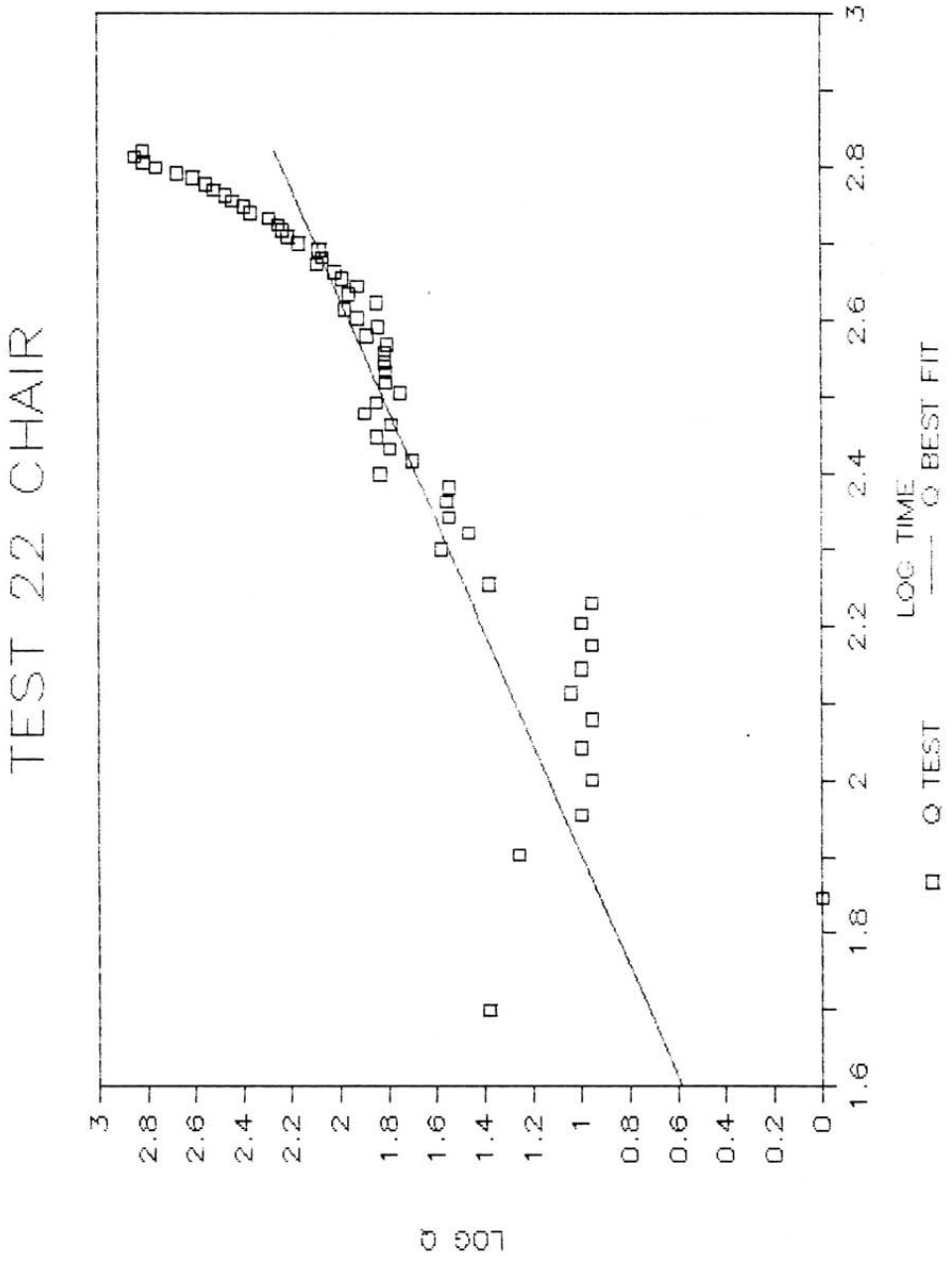
TEST 22 CHAIR
LOG Q
LOG TIME
Q TEST
Q BEST FIT
3
2.8
2.6
2.4
2.2
2
1.8
1.6
1.4
1.2
1
0.8
0.6
0.4
0.2
0
1.6
1.8
2
2.2
2.4
2.6
2.8
3

FIGURE 5

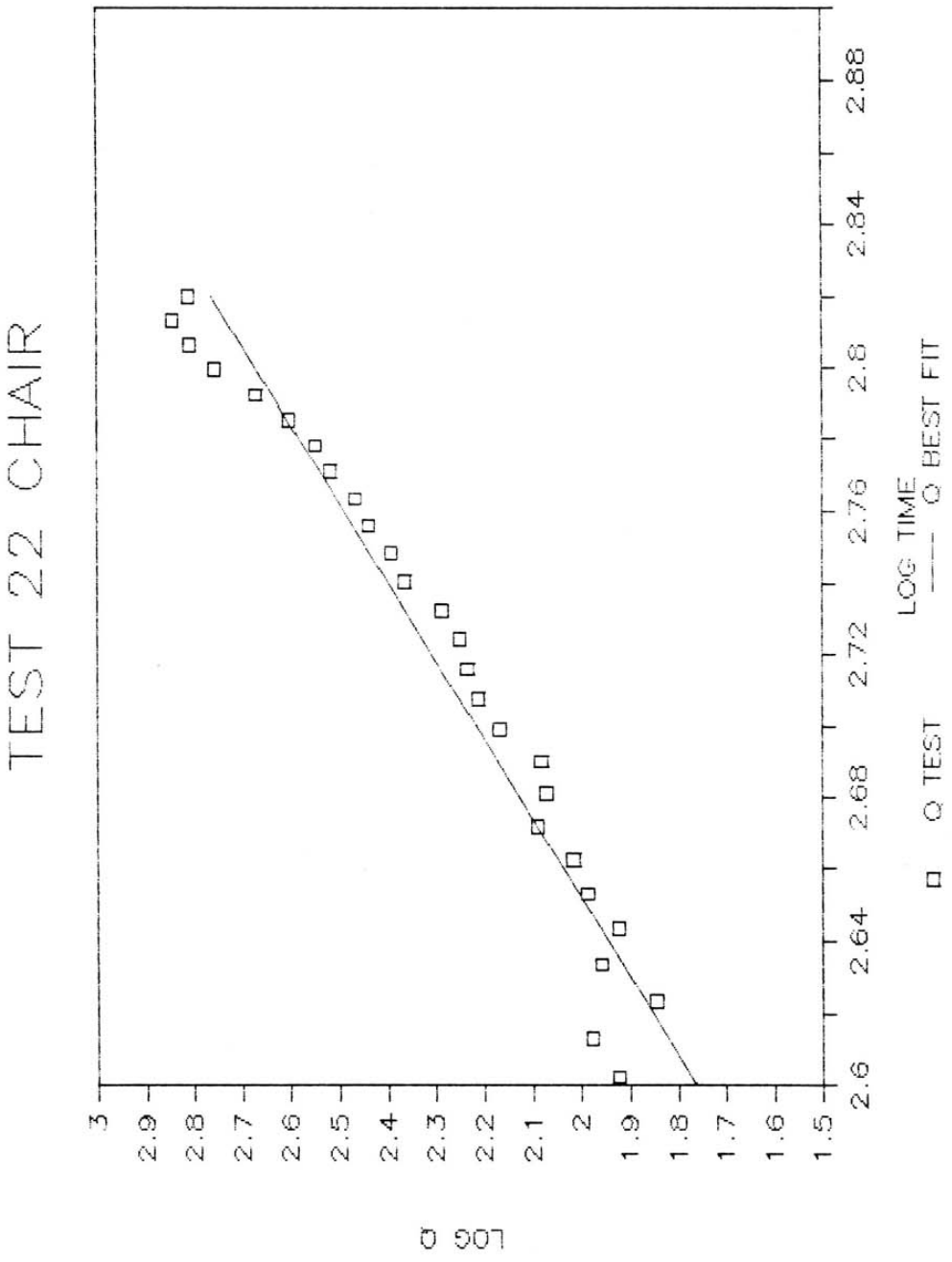
TEST 22 CHAIR
LOG Q
3
2.9
2.8
2.7
2.6
2.5
2.4
2.3
2.2
2.1
2
1.9
1.8
1.7
1.6
1.5
2.6
2.64
2.68
2.72
2.76
2.8
2.84
2.88
LOG TIME
Q TEST
Q BEST FIT

which radiation from the flame is the dominant means of heat transfer back to the fuel. Obviously this point will vary from fuel to fuel and will be dependent on many factors. The rigid definition of the virtual origin is beyond the scope of this thesis.

The selection of a virtual origin for regression analysis will depend on which part of the fire you are trying to model. Fitting the model to only part of the data produces errors. The magnitude and implications of these errors are discussed later.

For Test 22 the regression analysis from t_v = 400 to the peak at t = 660 seconds produced an exponent equal to 4.56 to be used in the power-law model. This is more than twice as large as the p = 2 used in Heskestad and Delichatsios' equations. The next step is determine if a p = 2, power-law model can be fit to the data.

Figure 6 shows heat release rate vs time data for Test 22 plotted on an x-y graph. The best fit power-law curve, based on t_v = 400, with alpha = 8 x 10^{-11} kW/sec^2 and p = 4.56 is superimposed. A curve based on the power-law model, $Q = at^2$, is also plotted. The value of alpha was varied until the p = 2 model assumed the same general shape as the test curve. In this case alpha equals 0.0086 kW/sec^2. The heat release rate for the p = 2 model was calculated beginning at t = 0, then plotted beginning at t = t_v = 400

FIGURE 6

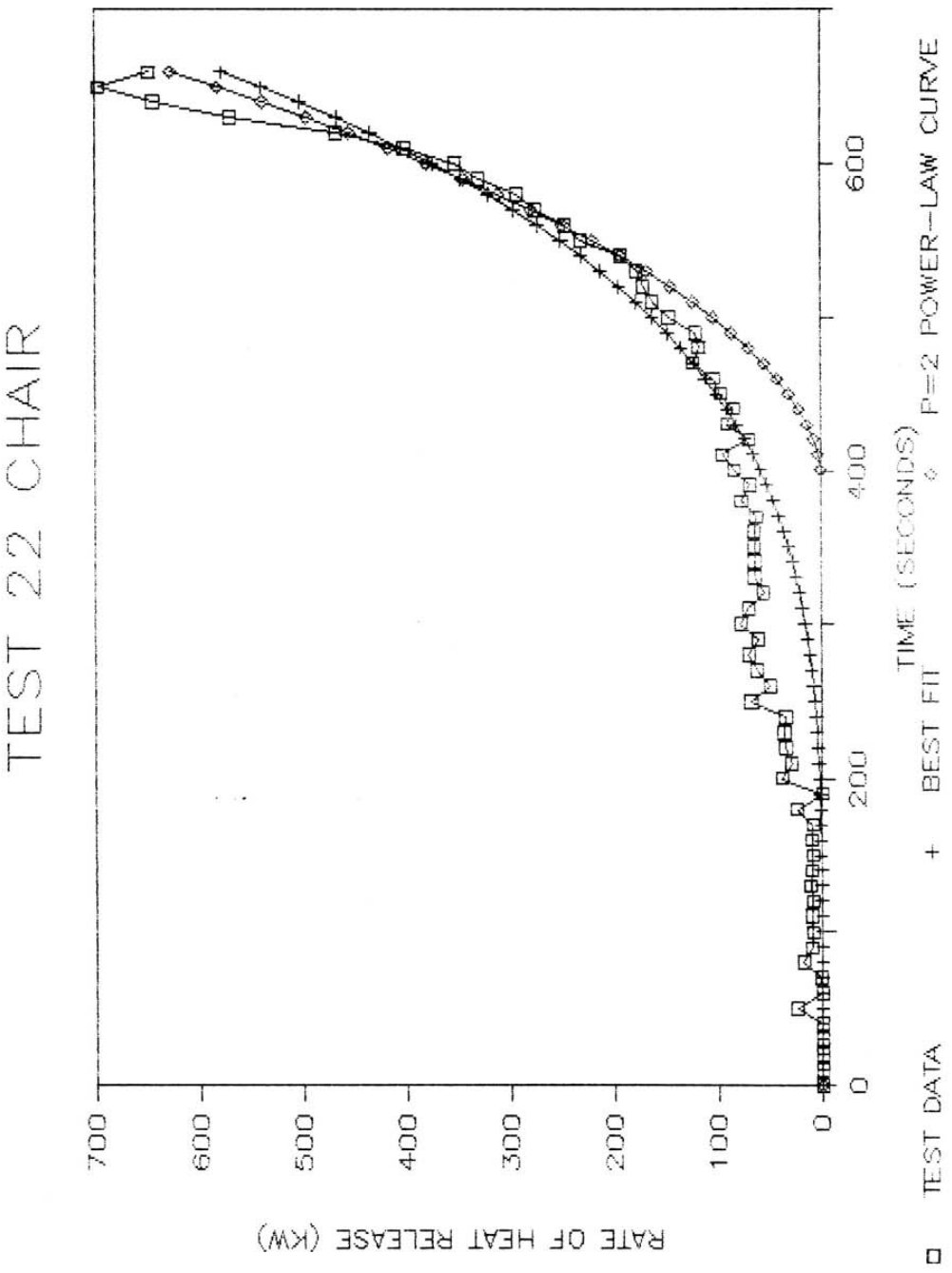
TEST 22 CHAIR
RATE OF HEAT RELEASE (KW)
0
100
200
300
400
500
600
700
0
200
400
600
TIME (SECONDS)
□ TEST DATA
+ BEST FIT
◇ P=2 POWER-LAW CURVE

seconds. By varying alpha and t_v, the p = 2 model can be forced to fit the data. Because the heat release rate was calculated beginning at t = 0, but plotted beginning at t = 400, this curve does not plot as a straight line on a log-log plot. Regression analyses were not used to determine the virtual origin or alpha for the p = 2 model. The effects of errors resulting from the arbitrary selection of alpha and t_v are discussed later.

Figure 6 shows that, initially, the best fit curve is a better approximation of the actual test data. After about 600 seconds the p = 2 power-law model is a better approximation of the data.

Figures 7 through 13 are plots of several NBS calorimeter tests along with best fit power-law curves and p = 2 models superimposed. Table 3 is a summary of the factors (alpha, t_v and p) used to generate the curves. The regression analyses and the procedures used to establish these curves were the same as those used in the example for Test 22.

For Test 67, two regression analyses were done, one with t_v = 90 seconds and one with t_v = 400 seconds. This was done to demonstrate that different realms of a fire can be modeled with different curves. The resulting curves are plotted in Figures 12 and 13. The errors resulting from the use of the

FIGURE 7

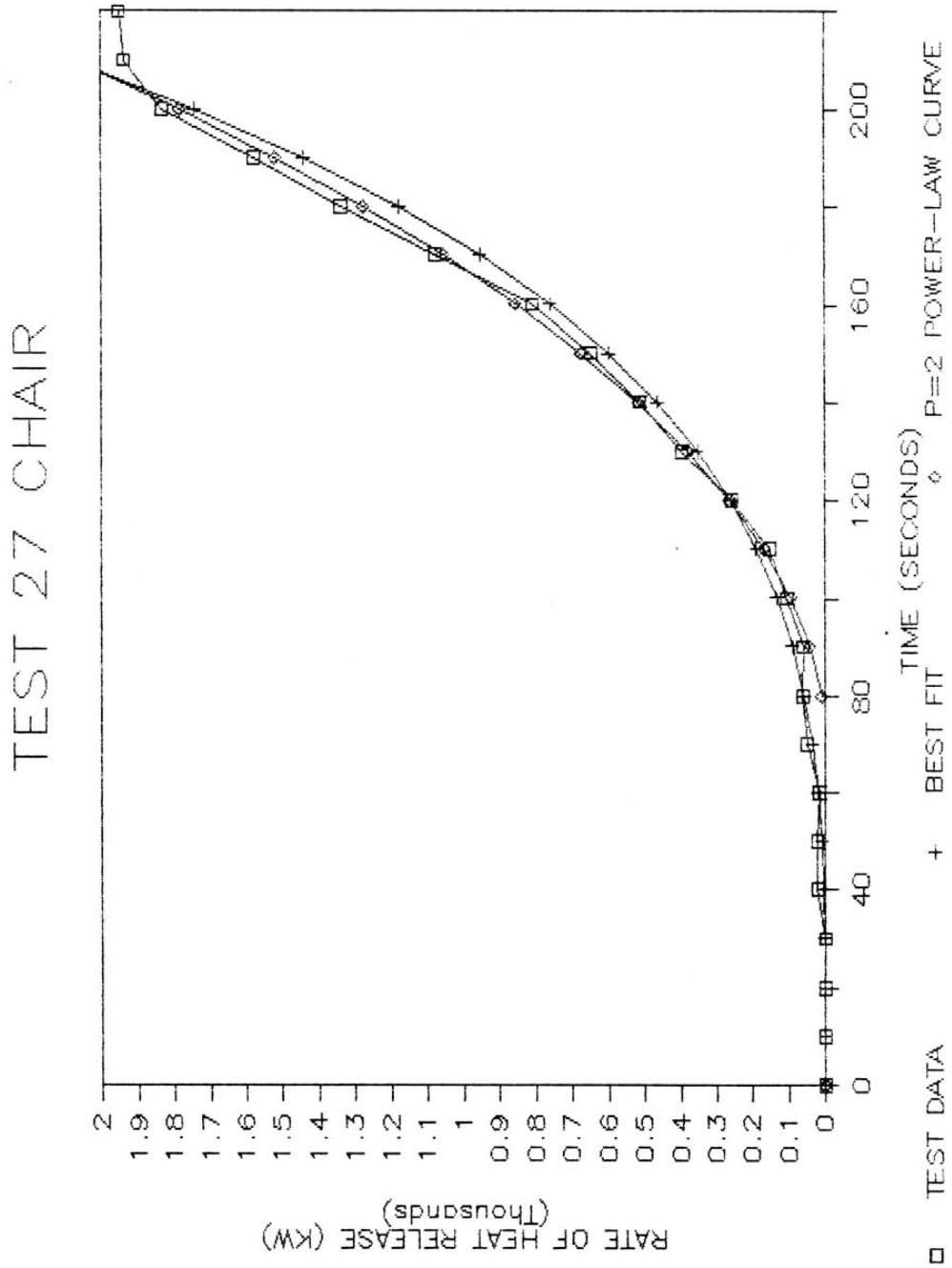
TEST 27 CHAIR
RATE OF HEAT RELEASE (kW)
(Thousands)
2
1.9
1.8
1.7
1.6
1.5
1.4
1.3
1.2
1.1
1
0.9
0.8
0.7
0.6
0.5
0.4
0.3
0.2
0.1
0
0
40
80
120
160
200
TIME (SECONDS)
□ TEST DATA
+ BEST FIT
◇ P=2 POWER-LAW CURVE

FIGURE 8

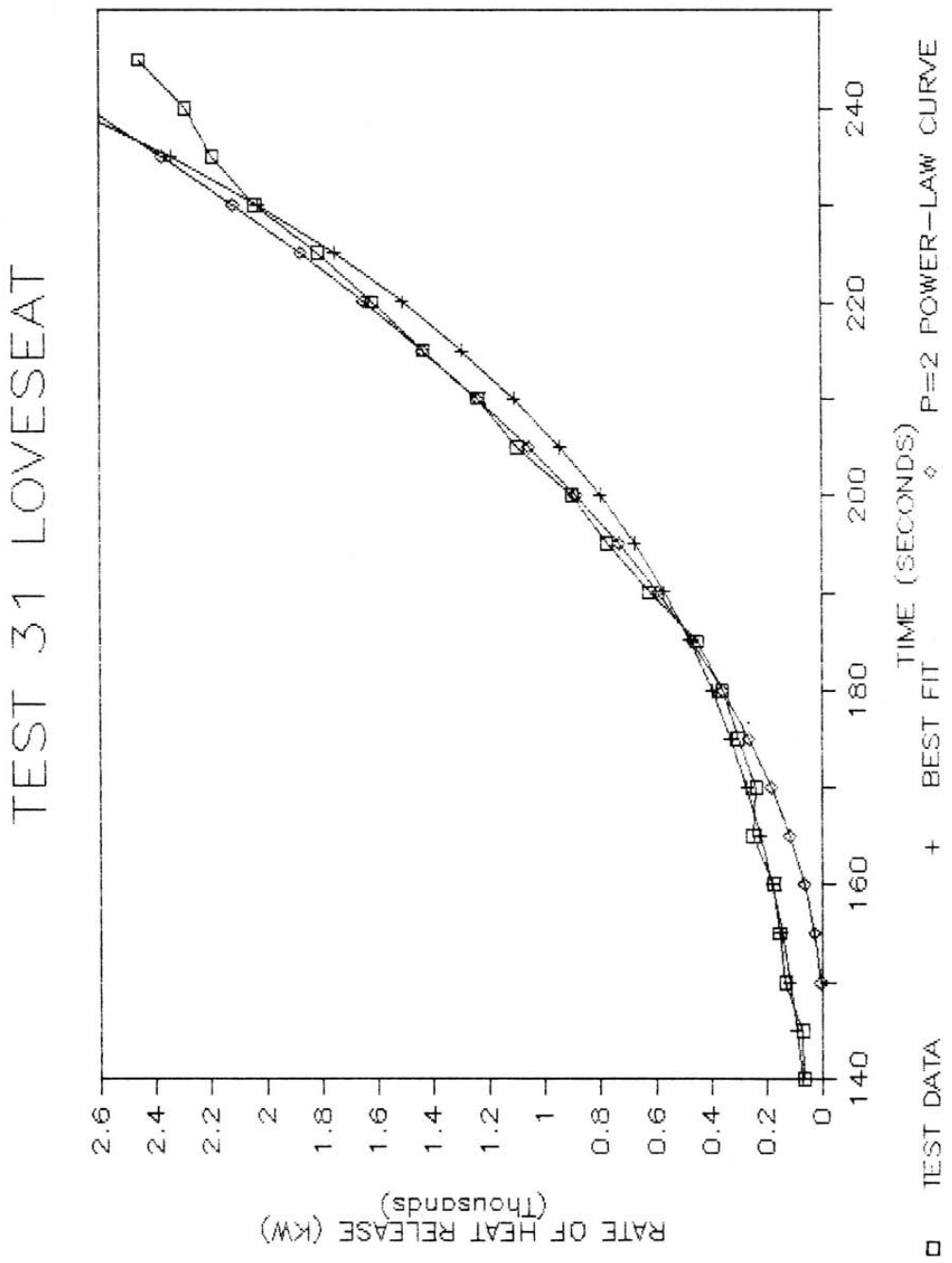
TEST 31 LOVESEAT
RATE OF HEAT RELEASE (kW)
(Thousands)
2.6
2.4
2.2
2
1.8
1.6
1.4
1.2
1
0.8
0.6
0.4
0.2
0
140
160
180
200
220
240
TIME (SECONDS)
□ TEST DATA
+ BEST FIT
◇ P=2 POWER-LAW CURVE

FIGURE 9

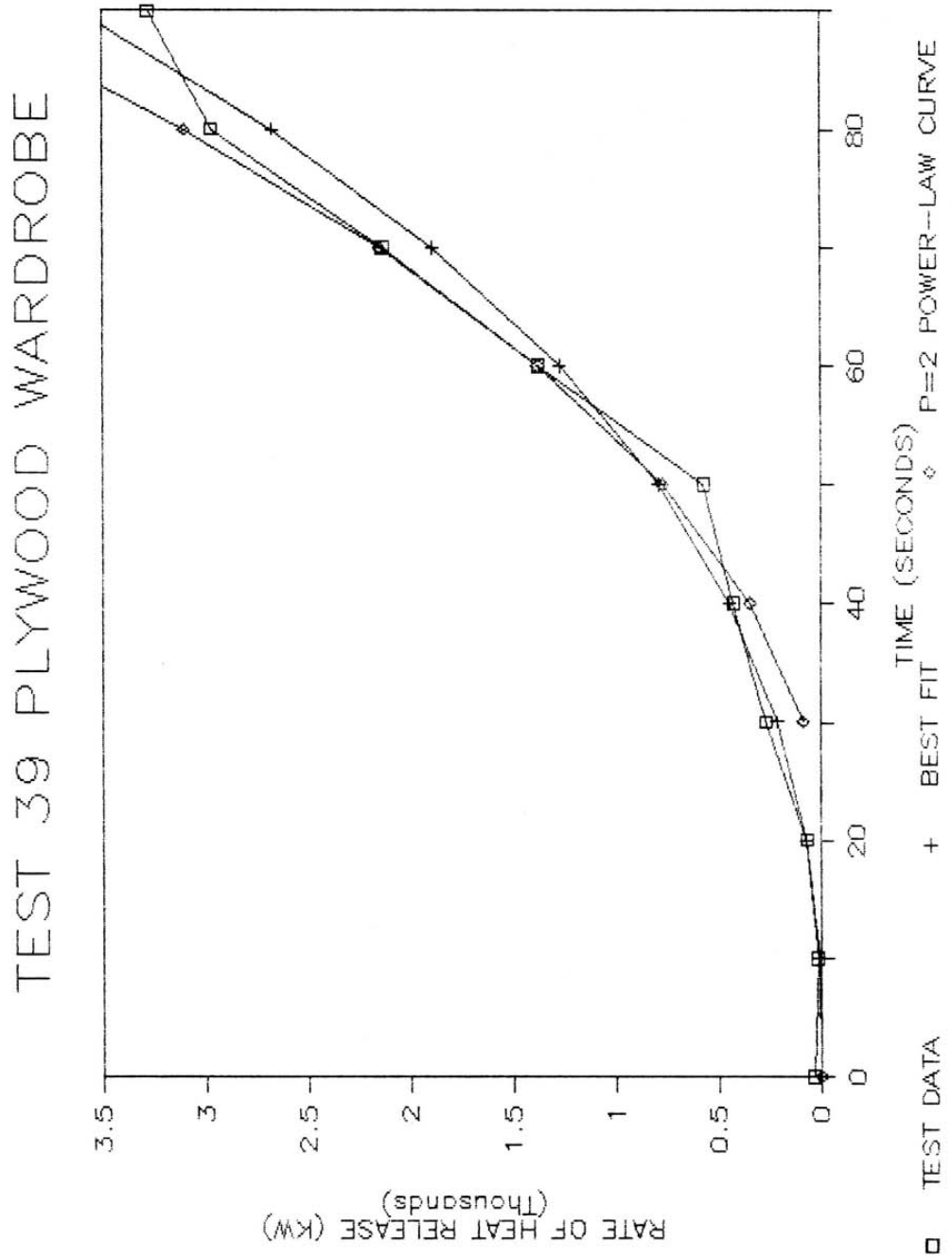
TEST 39 PLYWOOD WARDROBE
RATE OF HEAT RELEASE (KW)
(Thousands)
3.5
3
2.5
2
1.5
1
0.5
0
0
20
40
60
80
TIME (SECONDS)
□ TEST DATA
+ BEST FIT
◇ P=2 POWER-LAW CURVE

FIGURE 10

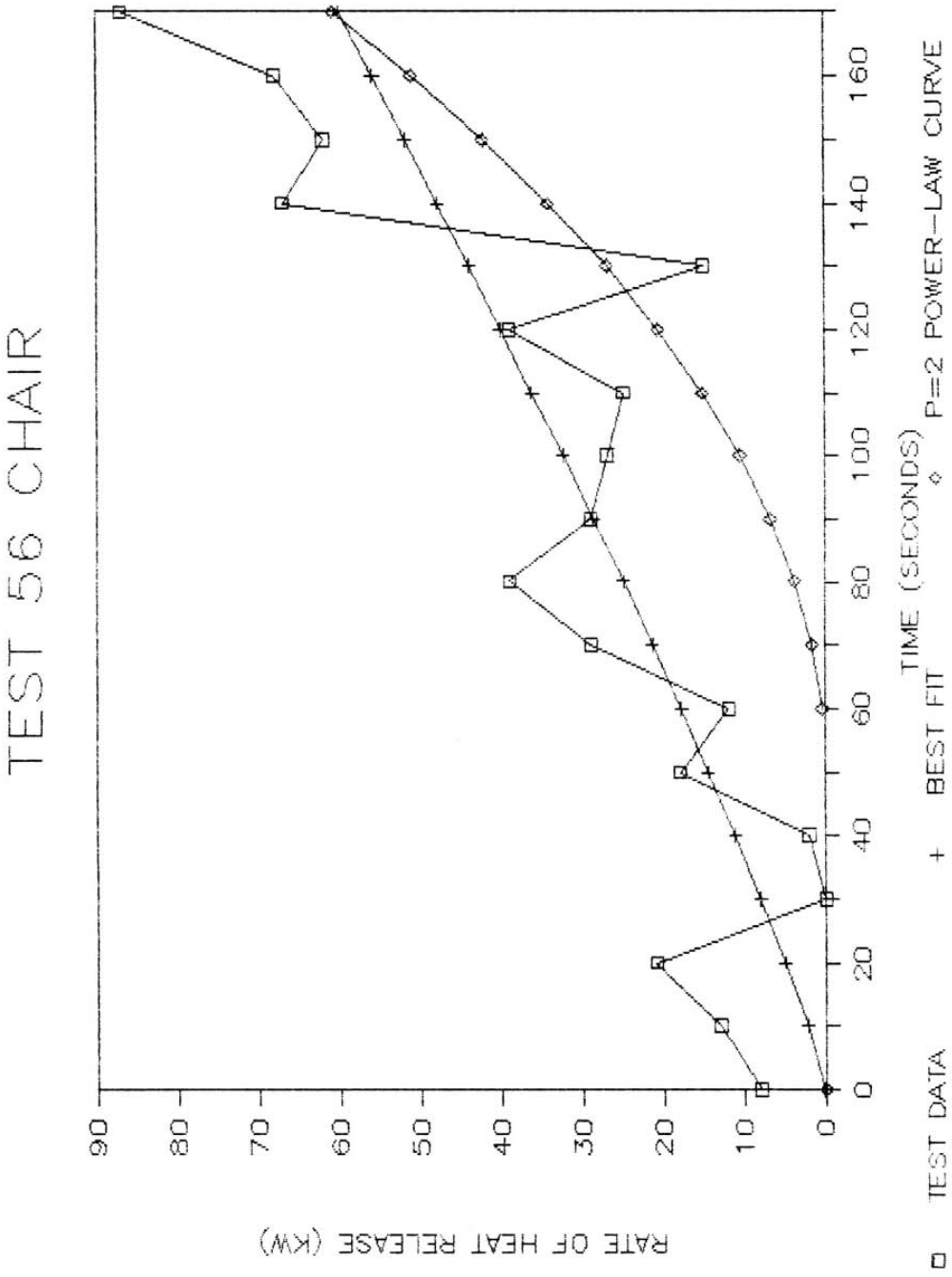
TEST 56 CHAIR
RATE OF HEAT RELEASE (KW)
0
10
20
30
40
50
60
70
80
90
0
20
40
60
80
100
120
140
160
TIME (SECONDS)
□ TEST DATA
+ BEST FIT
◇ P=2 POWER-LAW CURVE

FIGURE 11

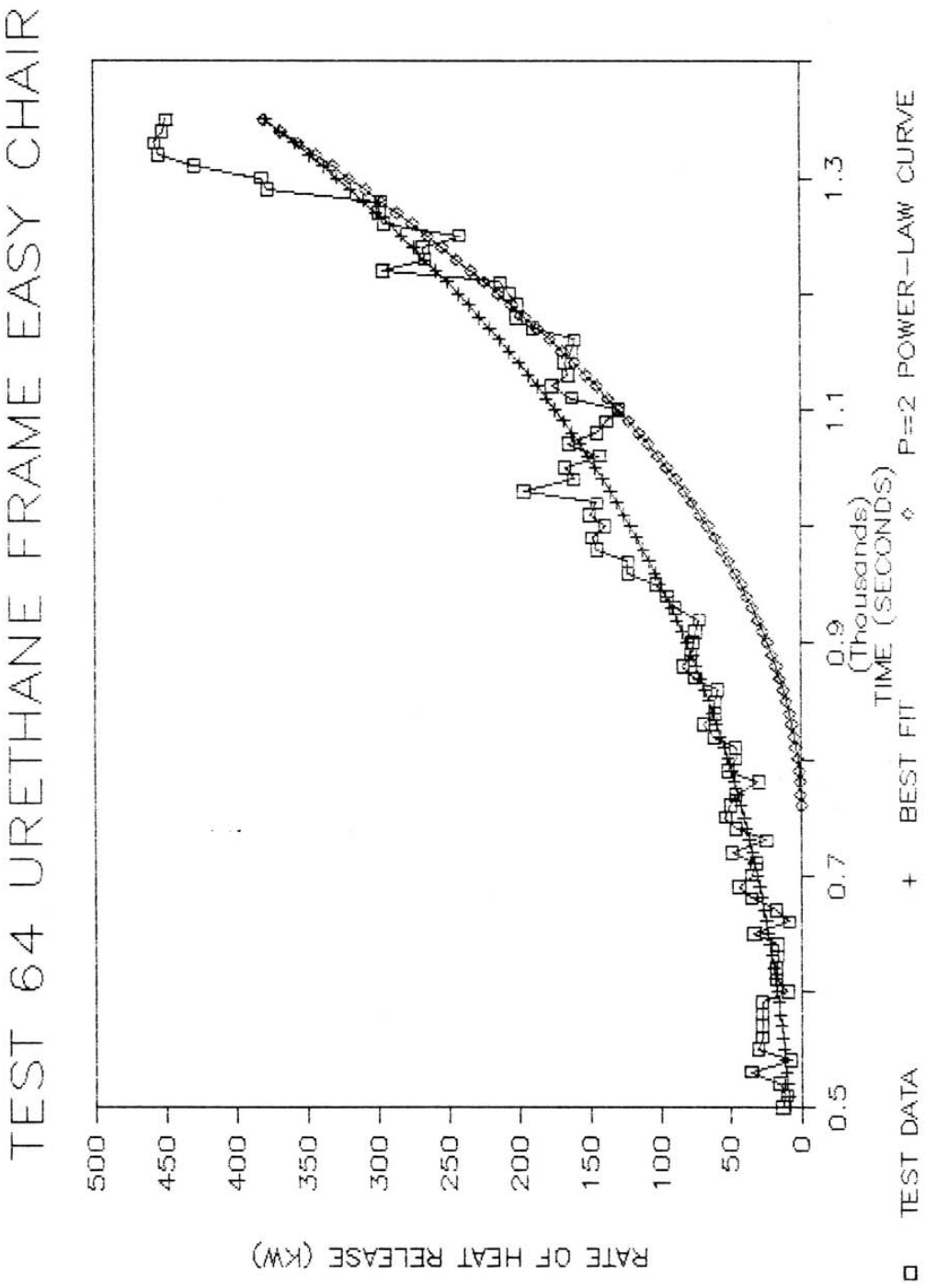
TEST 64 URETHANE FRAME EASY CHAIR
RATE OF HEAT RELEASE (KW)
500
450
400
350
300
250
200
150
100
50
0
0.5
0.7
0.9
1.1
1.3
(Thousands)
TIME (SECONDS)
□ TEST DATA
+ BEST FIT
◇ P=2 POWER-LAW CURVE

FIGURE 12

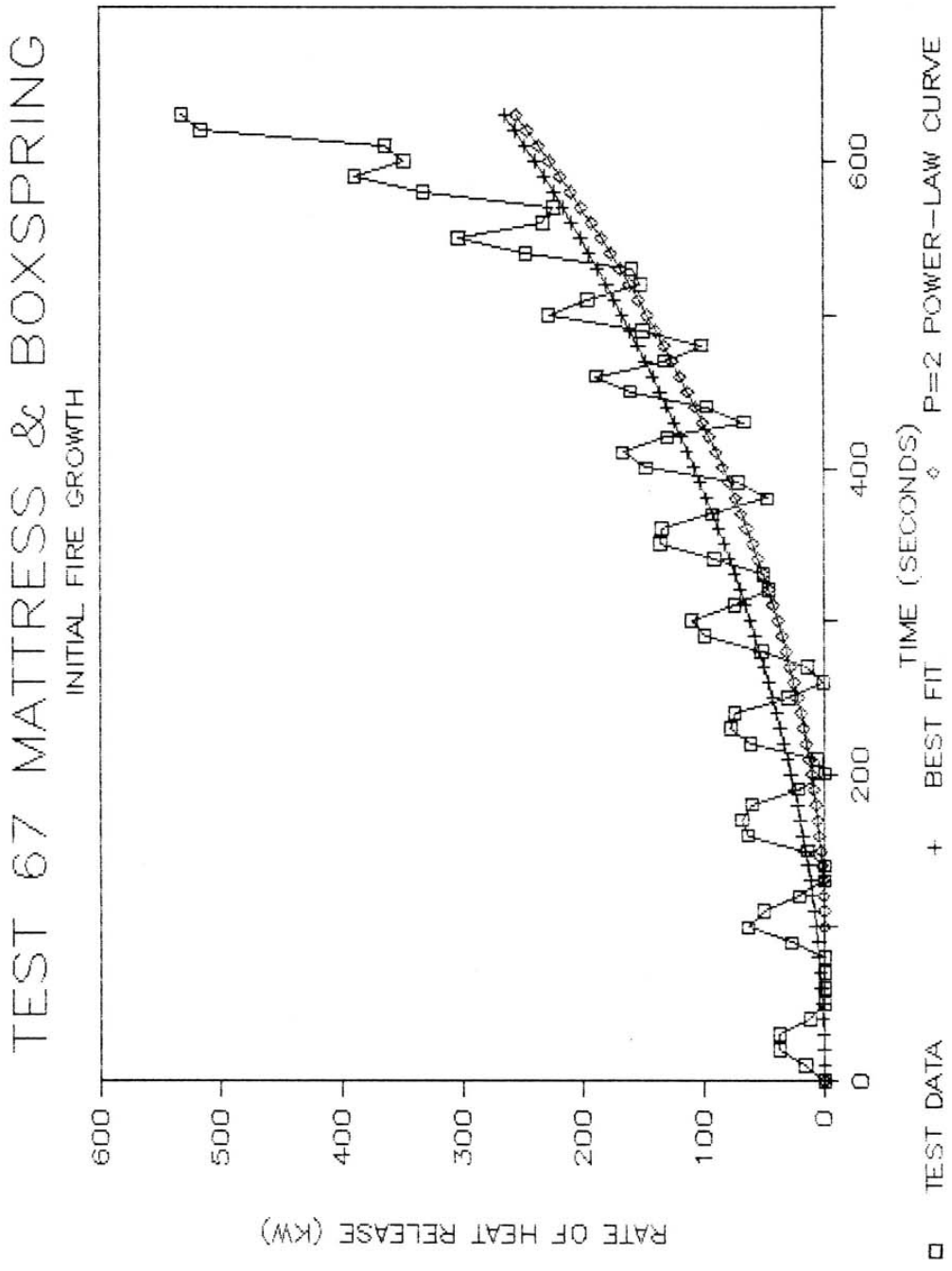
TEST 67 MATTRESS & BOXSPRING
INITIAL FIRE GROWTH
RATE OF HEAT RELEASE (KW)
600
500
400
300
200
100
0
0
200
400
600
TIME (SECONDS)
□ TEST DATA
+ BEST FIT
◇ P=2 POWER-LAW CURVE

FIGURE 13

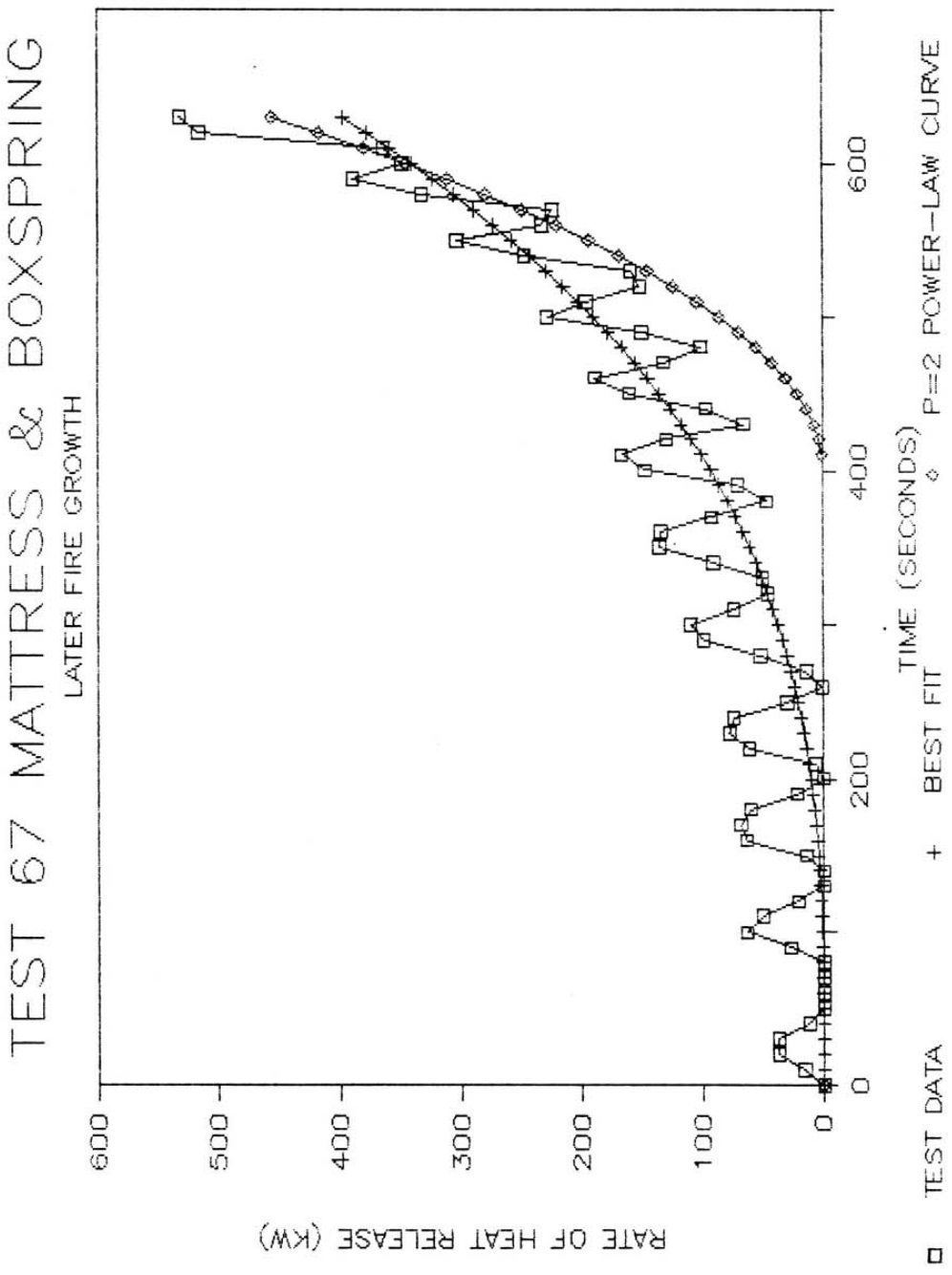
TEST 67 MATTRESS & BOXSPRING
LATER FIRE GROWTH
RATE OF HEAT RELEASE (KW)
600
500
400
300
200
100
0
0
200
400
600
TIME (SECONDS)
□ TEST DATA
+ BEST FIT
◇ P=2 POWER-LAW CURVE

TABLE 3

Test 22

Peak heat release rate: 648 kW at t = 660 seconds

For t = 0 to peak: alpha = 0.0241 kW/sec^2 p = 1.3762

For t = 400 to peak: alpha = $8x10^{-11}$ kW/sec^2 p = 4.5600

Using p = 2: alpha = 0.0086 kW/sec^2

Test 27

Peak heat release rate: 1951 kW at t = 220 seconds

For t = 0 to peak: alpha = 0.0334 kW/sec^2 p = 1.8586

For t = 70 to peak: alpha = $5x10^{-6}$ kW/sec^2 p = 3.7105

Using p = 2: alpha = 0.1055 kW/sec^2

Test 31

Peak heat release rate: 2456 kW at t = 245 seconds

For t = 0 to peak: alpha = 0.0175 kW/sec^2 p = 1.7076

For t = 145 to peak: alpha = $4x10^{-13}$ kW/sec^2 p = 6.6652

Using p = 2: alpha = 0.2931 kW/sec^2

Test 39

Peak heat release rate: 3278 kW at t = 90 seconds

For t = 0 to peak: alpha = 0.1140 kW/sec^2 p = 1.1349

For t = 20 to peak: alpha = 0.0331 kW/sec^2 p = 2.5784

Using p = 2: alpha = 0.8612 kW/sec^2

TABLE 3 CONTINUED

Test 56

Peak heat release rate: 87 kW at t = 170 seconds

For t = 0 to peak: alpha = 2.8669 kW/sec^2 p = 0.48316

For t = 50 to peak: alpha = 0.1553 kW/sec^2 p = 1.1598

Using p = 2: alpha = 0.0042 kW/sec^2

Test 64

Peak heat release rate: 457 kW at t = 1330 seconds

For t = 0 to peak: alpha = 0.0450 kW/sec^2 p = 1.0491

For t = 750 to peak: alpha = $5x10^{-10}$ kW/sec^2 p = 3.7941

Using p = 2: alpha = 0.0011 kW/sec^2

Test 67

Peak heat release rate: 532kW at t = 630 seconds

For t = 0 to peak: alpha = 0.1580 kW/sec^2 p = 1.0504

For t = 90 to peak: alpha = 0.0008 kW/sec^2 p = 1.9630

Using p = 2: alpha = 0.0009 kW/sec^2

For t = 400 to peak: alpha = $5x10^{-7}$ kW/sec^2 p = 3.1858

Using p = 2: alpha = 0.0086 kW/sec^2

regression curves or the p = 2 power-law models, as opposed to the actual test data, are discussed later in terms the effects on the design and analysis of detector response.

Appendix A contains a set of graphs for forty furniture calorimeter tests along with p = 2 power-law curves superimposed. Alpha and t_v were not calculated using regression techniques, but were simply varied until the fits appeared to be good. In many cases a smaller t_v can be used to produce an even better fit to the data. The use of the larger t_v will result in designs of detection systems which are conservative. The effects of this are discussed later in terms of the effects on predicted fire size, response time and required detector spacing. As with Test 67, for several of the tests there are more than one graph. Table 4 is summary of the test and power-law data contained in the appendix.

In all but one test the p = 2, power-law fire growth model could be used to simulate the initial growth of the fire. Test Number 55 (Figure 38 of Appendix A), a metal frame chair with a padded seat never burned at a rate greater than 13 kW. This type of a fire would fail to activate a fire detector or a sprinkler unless the detector was very close to the fire. At such low heat outputs, random convective forces would be as great as the velocities due to the buoyant flow.

In each of the other test cases it was possible to

TABLE 4

SUMMARY OF DATA USED TO PRODUCE POWER-LAW, P = 2 CURVES TO FIT NBS CALORIMETER TESTS

FIG. NO.	TEST NO.	CRITICAL TIME SECONDS		ALPHA KW/SEC SQ.	VIRTUAL TIME SECONDS	PAGE
Al	TEST	15	50	0.4220	10	1ll
A2	TEST	18	400	0.0066	140	112
A3	TEST	19	175	0.0344	110	113
A4	TEST	19	50	0.4220	190	114
A5	TEST	21	250	0.0169	10	115
A6	TEST	21	120	0.0733	60	116
A7	TEST	21	100	0.1055	30	117
AS	TEST	22	350	0.0086	400	118
A9	TEST	23	400	0.0066	100	119
A10	TEST	24	2000	0.0003	150	120
All	TEST	25	200	0.0264	90	121
A12	TEST	26	200	0.0264	360	122
A13	TEST	27	100	0.1055	70	123
A14	TEST	28	425	0.0058	90	124
A15	TEST	29	60	0.2931	175	125
A16	TEST	29	100	0.1055	100	126
A17	TEST	30	60	0.2931	70	127
A18	TEST	31	60	0.2931	145	128
A19	TEST	37	80	0.1648	100	129
A20	TEST	38	100	0.1055	50	130
A21	TEST	39	35	0.8612	20	131
A22	TEST	40	35	0.8612	40	132
A23	TEST	41	40	0.6594	40	133
A24	TEST	42	70	0.2153	50	134
A25	TEST	42	30	1.1722	100	135
A26	TEST	43	30	1.1722	50	136
A27	TEST	44	90	0.1302	30	137
A28	TEST	45	100	0.1055	120	138
A29	TEST	46	45	0.5210	130	139
A30	TEST	47	170	0.0365	30	140
A31	TEST	48	175	0.0344	90	141
A32	TEST	49	200	0.0264	50	142
A33	TEST	50	200	0.0264	120	143
A34	TEST	51	120	0.0733	20	144
A35	TEST	52	275	0.0140	2090	145
A36	TEST	53	350	0.0086	50	146
A37	TEST	54	500	0.0042	210	147
A38	TEST	55				148
A39	TEST	56	500	0.0042	50	149
A40	TEST	57	350	0.0086	500	150
A41	TEST	61	150	0.0469	0	151
A42	TEST	62	65	0.2497	40	152
A43	TEST	64	1000	0.0011	750	153
A44	TEST	66	75	0.1876	3700	154
A45	TEST	67	350	0.0086	400	155
A46	TEST	67	1100	0.0009	90	156

obtain a p = 2, power-law curve to model the fire growth. In five cases the test specimens exhibited different realms of burning. Each of the realms is modeled by different power-law fire growth curves as was shown above for Test 67. These tests are numbers 19, 21, 29, 42 and 67.

Figures 14 and 15 are of NBS Test Number 19. This chair had a wood frame and was covered with a polyurethane foam padding. The fabric covering this typical easy chair was a polyolefin fabric. The first graph shows the initial stage of the fire growth in Test 19. The second graph shows the complete development of the fire.

If interested in the initial growth of this type of fire, it can be modeled with the curve shown in Figure 14. This graph shows that the heat release rate of the fire increases rapidly at about 140 seconds after ignition. At about 200 seconds the chair is burning at a rate of 300 kW (284 BTU/sec). To model the fire growth, use:

$$Q_p\ (kW) = a(kW/sec^2)(t - t_v)^2(sec^2) \qquad [20]$$

or:

$$Q_p\ (kW) = [1055\ (kW)/t_c^2(sec)]\ (t - t_v)^2(sec) \qquad [21]$$

With:

$a = 0.0344\ kW/sec^2$ or $t_c = 175$ sec

$t_v = 110$ sec

FIGURE 14

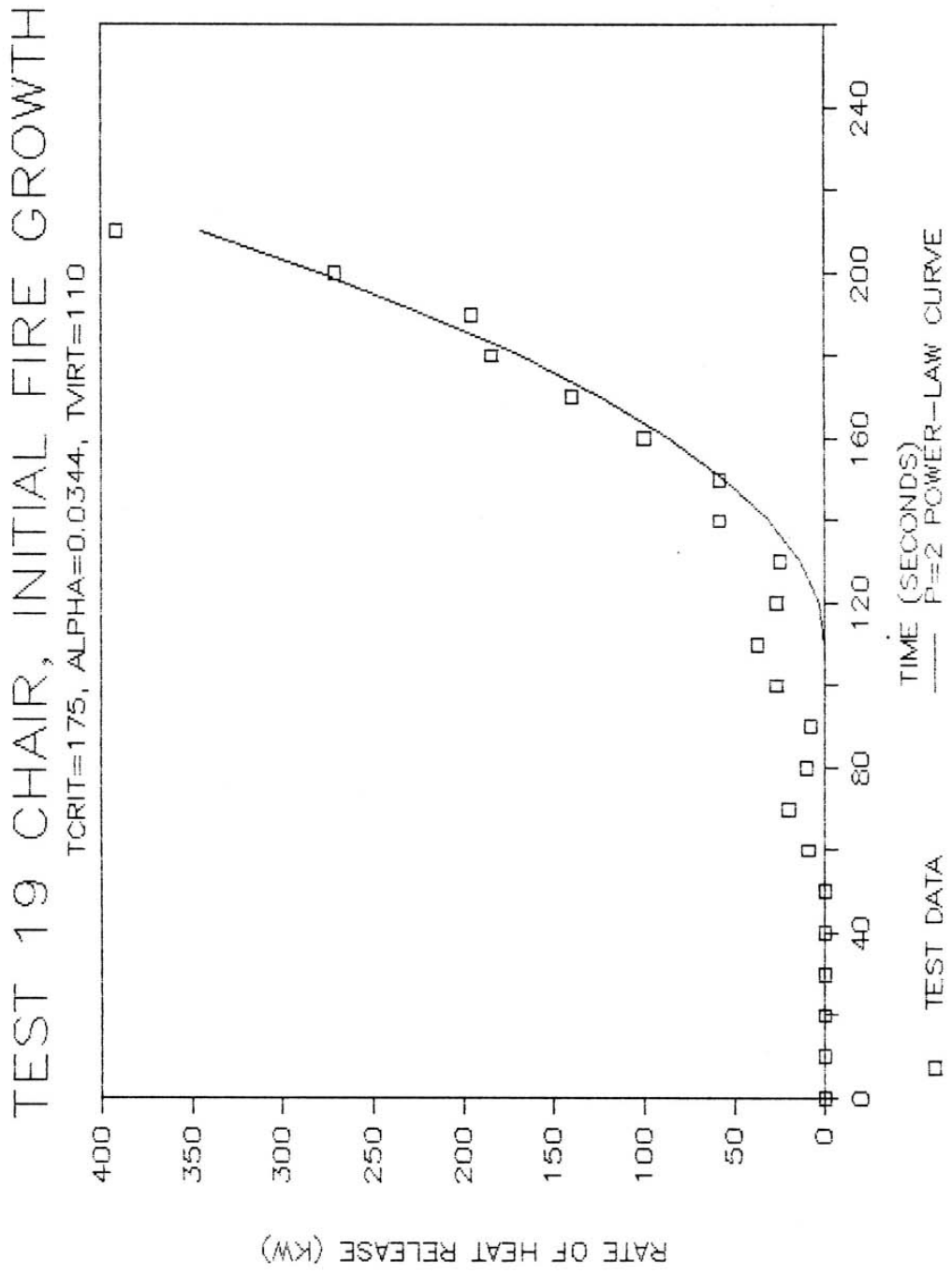
TEST 19 CHAIR, INITIAL FIRE GROWTH
TCRIT=175, ALPHA=0.0344, TVIRT=110
RATE OF HEAT RELEASE (KW)
400
350
300
250
200
150
100
50
0
0
40
80
120
160
200
240
TIME (SECONDS)
TEST DATA
P=2 POWER-LAW CURVE

FIGURE 15

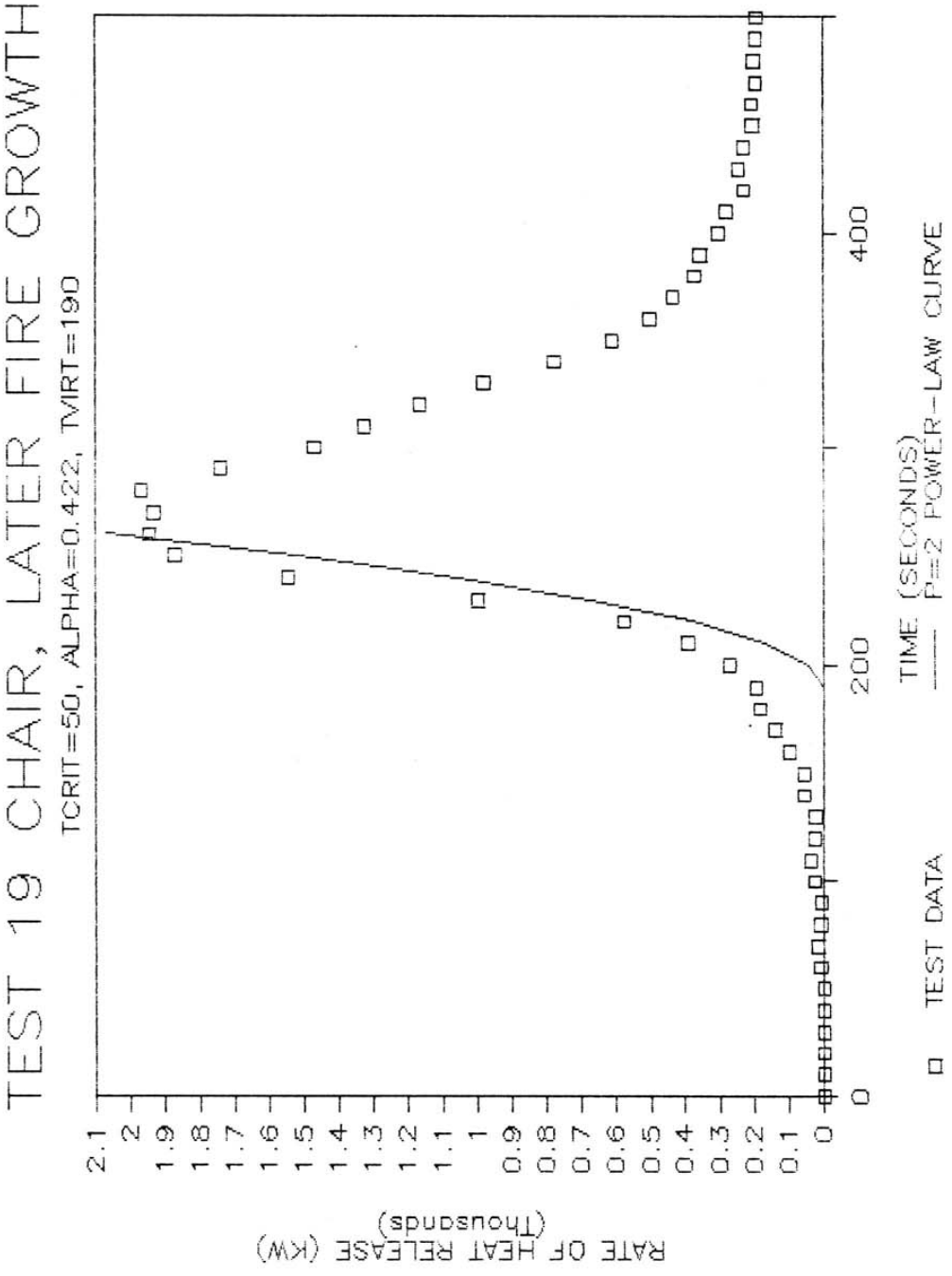
TEST 19 CHAIR, LATER FIRE GROWTH
TCRIT=50, ALPHA=0.422, TMRT=190
RATE OF HEAT RELEASE (KW)
(Thousands)
2.1
2
1.9
1.8
1.7
1.6
1.5
1.4
1.3
1.2
1.1
1
0.9
0.8
0.7
0.6
0.5
0.4
0.3
0.2
0.1
0
0
200
400
TIME (SECONDS)
TEST DATA
P=2 POWER-LAW CURVE

To make the p = 2, power-law curve fit, it must have a virtual origin of 110 seconds. This causes the curve to fit the actual data after about 140 to 150 seconds. Between 110 and 140 seconds, the temperature and velocity of the gases predicted by the equations developed by Heskestad and Delichatsios would be slightly in error. The error would be on the conservative side when the equations are used to design a detection system. This is because the predicted heat release rate is slightly below the actual measured value at a given time. The model will then predict lower temperatures and velocities in the fire plume and across the ceiling. This causes a fire detector or sprinkler, located a distance r and a height H from the fire, to respond sooner to the real fire than to the model.

If a latter stage in the development of the fire is of interest, Figure 15 shows a model curve which could be used. This burning realm of Test 19 is modeled by a p = 2 power-law growth with alpha = 0.422 (kW/sec^2) and a virtual origin of 190 seconds.

The graphs of the forty tests show that the power-law fire growth model, $Q = at^p$, with p = 2 can be used to model different stages of the initial development of the furniture calorimeter fires. The main difficulty arises when trying to select the proper value for the fire growth parameter, alpha. As more data becomes available from furniture calorimeter

tests and other fire tests, fire protection engineers will be better able to make estimates of alpha for furnishings and commodities in an area they might be studying.

Appendix A is a catalog of fire growth parameters for different fuels. Engineers can use it to select the approximate fire growth characteristics necessary to model similar fuel packages using Heskestad and Delichatsios' equations or the graphs and tables of NFPA 72-E, Appendix C. The data contained in Appendix A is best used in conjunction with the original NBS reports on the calorimeter tests (References 12 and 16). In addition to heat release rate, the NBS reports contain data such as rate of mass loss, particulate conversion and target irradiance, plotted as a function of time.

Appendix A shows that a p = 2, power-law model can be used to model open air furniture fires. As shown above, a regression analysis can be done to determine the exponent and the alpha which best fit the test data. However, the objective here is to show how engineers can use the p = 2 power-law equations proposed by Heskestad and Delichatsios to design and analyze detector response. The effects of using p = 2 are discussed later.

5. RESPONSE MODEL FOR HEAT DETECTORS AND AUTOMATIC SPRINKLERS

The power-law fire growth model combined with the similarity equations proposed by Heskestad and Delichatsios, defines the environment of a sprinkler or fire detector in terms of the temperature and velocity of fire gases across the ceiling. The relationship found in the Factory Mutual test data between optical density and the change in temperature at a point, can be used to estimate the optical density as a function of time during the initial growth of the fire. The next step is to combine these relationships with models which define the response of commercially available sprinklers and fire detectors.

Table 5 is a cross reference of fire signatures and commercially available detector types. The table shows which units respond to the various fire signatures listed. It should be noted that the detector types which respond to heat are also affected by infrared or thermal radiation. However in the initial stages of fire growth, convective heating by the fire gases will be the predominant means of heat transfer. In addition, because most sprinklers and fire detectors have a relatively small surface area and respond at temperatures below 300 degrees Fahrenheit, the radiation to and from the units can ignored when calculating their response.

TABLE 5
FIRE SIGNATURES AND COMMERCIALLY AVAILABLE DETECTORS

FIRE SIGNATURE / DETECTOR TYPE	ELECTROMAGNETIC RADIATION WAVE LENGTH 1700 TO 2900 ANGSTROMS	ELECTROMAGNETIC RADIATION (THERMAL) 6500 - 8500	INVISIBLE PRODUCTS OF COMBUSTION LESS THAN .1 MICRON	VISIBLE SMOKE AND PRODUCTS OF COMBUSTION MORE THAN .1 MICRON	RATE OF RISE IN TEMPERATURE	HIGH TEMPERATURE	
ULTRAVIOLET DETECTOR	X						
INFRARED DETECTOR		X					
SMOKE DETECTOR							
PHOTOELECTRIC				X			
IONIZATION			X				
PHOTO BEAM				X			
RATE OF RISE HEAT DETECTOR					X		
RATE ANTICIPATION HEAT DETECTOR						X	
FIXED TEMPERATURE HEAT DETECTOR						X	

The response of ultraviolet and infrared fire detectors can not be modeled directly using Heskestad and Delichatsios's fire model. The response of these detector types is beyond the scope of this paper.

Figure 16 describes the heat transfer taking place between a heat detector or sprinkler and its environment. The total heat transfer rate to the unit, q_{total}, can be described by:

$$q_{total} = q_{cond} + q_{conv} + q_{rad} \text{ (BTU/sec or kW)} \quad [22]$$

Where q_{cond}, q_{conv} and q_{rad} represent conduction, convection and radiation heat transfer rates respectively. As was previously discussed, during the initial realm of fire growth, radiation heat transfer can be neglected. Since the elements of most commercially available heat detectors and sprinklers are thermally isolated from the remainder of the unit, it is logical to assume that the heat lost from the detector or sprinkler element, by conduction to other parts of the detector and to the ceiling, is negligible in comparison to the convection heat transfer taking place. This leaves a net rate of heat transfer to the detector equal to q_{conv}. The convective heat transfer rate to the detector is described by:

$$q = q_{conv} = hA(T_g - T_d) \text{ BTU/sec (kW)} \quad [23]$$

FIGURE 16

HEAT TRANSFER TO A CEILING MOUNTED DETECTOR

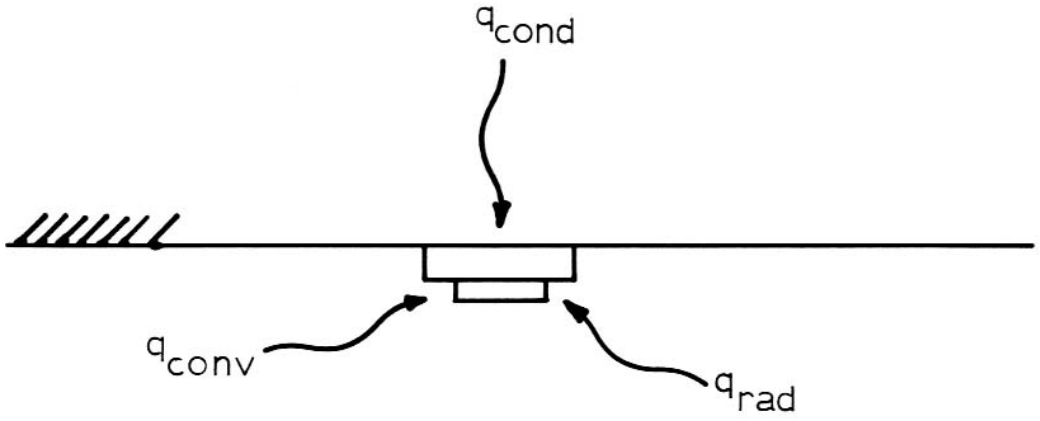

$$q_{total} = q_{cond} + q_{conv} + q_{rad}$$

The convective heat transfer coefficient is h and has units of BTU/(sec ft^2 °F) or kW/(m^2 °C). A is the area being heated. T_d and T_g are the detector temperature and the temperature of the gas heating the detector. Treating the detector element or sprinkler link as a lumped mass, m (lbm or kg), the change in its temperature is found by:

$$dT_d/dt = q/mc \quad \text{deg/sec} \qquad [24]$$

Where c [BTU/(lbm °F) or kJ/(kg °C)] is the specific heat of the element being heated. This leads to the following relationship for the change in temperature of the detector.

$$dT_d/dT = hA(T_g - T_d)/mc \qquad [25]$$

Heskestad and Smith [17] have proposed use of the following equation to describe the convective heat transfer to a particular detector element:

$$\Gamma = mc/hA \quad \text{seconds} \qquad [26]$$

$$dT_d/dT = (T_g - T_d)/\Gamma \qquad [27]$$

Note that Γ is a function of the mass, area and specific heat of the particular detector element being studied. For a given fire gas temperature and velocity and a particular detector or link design, an increase in mass increases Γ. A larger Γ results in slower heating of the element.

The convective heat transfer coefficient h, is a function of the velocity of the gases flowing past the detector element. For a given detector, if the gas velocity is constant, h is constant. It has been shown [18] that the convective heat transfer coefficient for spheres, cylinders and other objects similar to a sprinkler or heat detector element is approximately proportional to the square root of the Reynolds number, R_e.

$$R_e = ud/v \qquad [28]$$

Here, u is the gas velocity, d is the diameter of a cylinder or sphere exposed to convective heating and v is the kinematic viscosity of the gas. For a given detector this means that h and hence Γ, is proportional to the square root of the velocity of the gases passing the detector. This can be expressed as:

$$\Gamma u^{1/2} \sim= \Gamma_0 u_0^{1/2} = RTI \qquad [29]$$

Thus, if Γ_0 is measured in the laboratory at some reference velocity u_0, this expression is used to determine the Γ at any other gas velocity u, for that detector. The product, $\Gamma u^{1/2}$ is the Response Time Index, RTI.

Heskestad and Smith [17] developed a test apparatus at Factory Mutual to determine the RTI of sprinkler heads. In the test, called a plunge test, the sprinkler head is

suddenly lowered into the flow of a hot gas. The temperature and velocity of the gas are known and are constant during the test. The equation for the change in the detector temperature is then:

$$dT_d/dt = (1/\Gamma)(T_g - T_d) \qquad [30]$$

Since the gas temperature is constant during the test, the solution to this equation is:

$$T_d - T_a = (T_g - T_a)[1 - \exp(-t/\Gamma)] \qquad [31]$$

Where T_a is the ambient temperature or initial temperature of the sprinkler or detector. T_d is the temperature of the detector at time t. Rearranging the equation gives:

$$\Gamma = t/\ln[T_g - T_a)/(T_g - T_d)] \qquad [32]$$

By measuring the response time t_r, of the unit in the plunge test this equation can be used to calculate to at the test velocity u_0. This is done by substituting the response temperature and time for T_d and t. The sensitivity of the detector or sprinkler can then be expressed as:

$$\Gamma_0(\text{at } u_0) = t_r/\ln[T_g - T_a)/(T_g - T_r)] \ \text{(sec)} \qquad [33]$$

In terms of the Response Time Index this equation becomes:

$$RTI = t_r u_0^{1/2} / \ln[(T_g - T_a)/(T_g - T_r)] \quad [34]$$

The RTI has units of $ft^{1/2}sec^{1/2}$ or $m^{1/2}sec^{1/2}$.

A plunge test can be used to determine the RTI for a heat detector or a sprinkler. Knowing the RTI, the change in temperature of similar units can be calculated for any history of fire gases flowing past it. The form of the heat transfer equation is:

$$dT_d/dt = u^{1/2}(T_g - T_d)/RTI \quad [35]$$

This equation is used to calculate the temperature of a fixed temperature heat detector or sprinkler. The equation can be used to determine the time at which the unit reaches its operating temperature.

The use of a lumped mass model may not hold for rate of rise heat detectors and rate compensated heat detectors. The heat transferred to a fixed temperature heat detector heats a sensing element until it melts. The element itself is exposed to the hot gases. This is not true for rate of rise heat detectors or rate compensated heat detectors.

Most commercial rate of rise heat detectors operate when the expansion of air in a chamber exceeds the rate at which the air can escape through a small vent hole. For this type

of detector it is also necessary to model heat transfer from the detector body to the air in its chamber. Then the expansion of the air and its escape through a vent hole must be accounted for. The response time index determined in a plunge test may not be constant as fire gas velocities or temperatures vary.

A rate compensated detector consists of an metallic shell surrounding two bowed metal struts. There are electrical contacts on the struts. The struts and shell expand at different rates as the detector is heated. When heated fast the outer shell expands and causes the bowed struts to straighten and close the contacts, signaling an alarm. This usually occurs at temperatures below the rated operating temperature. However if the unit is heated more slowly, the difference between the expansion rates of the inner and outer parts is such that the contacts close at or near the units rated temperature.

Obviously, the rate compensated type of heat detector can not be treated as a lumped mass when calculating its response to a fire. As with rate of rise heat detectors, there are more heat transfer components to the response formula than a simple lumped mass.

More research must be done to determine good working response models for rate of rise and rate compensated heat

detectors. Some recent plunge tests [19] done on rate compensated heat detectors showed them to have low values of RTI at the temperatures and velocities of the tests. The effect of varying temperature and velocity was studied, but the data have not yet been analyzed and published [19].

It will be interesting to see how the RTI of a rate compensated or rate of rise detector changes when temperatures and velocities are varied. The error in using a constant value for the RTI might be small enough to have little or no effect on the precision of the response model.

The equations proposed by Heskestad and Delichatsios for the velocity and temperature of fire gases in the ceiling jet are inserted into the heat transfer equation to calculate the response of a detector. The nature of the equations for temperature and velocity presented thus far, are such that the integration of the heat transfer equation must be done numerically. This type of solution is inherently less precise than analytical integration and will require hundreds of iterations to obtain a good answer.

By going back to Heskestad's original work [20] and using a modified correlation of the data, Beyler [7] found an analytical method to integrate the similarity equations with the heat transfer equation. First the numerical solution will be presented. Then Beyler's analytical solution will be discussed.

6. NUMERICAL SOLUTION FOR DESIGNING SYSTEM RESPONSE

For convenience the relationships proposed by Heskestad and Delichatsios are repeated here along with the equation for the heat transfer to a detector or sprinkler.

$$a = 1000(\text{BTU/sec})/[t_c(\text{sec})]^2 \quad [36]$$

or:

$$t_c = [1000(\text{BTU/sec})/a]^{1/2} \quad [37]$$

$$t = (0.251 t_c^{2/5} H^{4/5}) t_2^* \quad [38]$$

$$DT = (15.8 t_c^{-4/5} H^{-3/5}) DT_2^* \quad [39]$$

$$u = (3.98 t_c^{-2/5} H^{1/5}) u_2^* \quad [40]$$

and:

$$t_{2f}^* = 0.75 + 0.78(r/H) \quad [41]$$

If $t_2^* \leq t_{2f}^*$ then: $DT_2^* = 0$

Else:

If $t_2^* > t_{2f}^*$ then:

$$t_2^* = t_{2f}^* + 2.22(DT_2^*/1000)^{0.781} + 3.69(DT_2^*/1000)^{0.870}(r/H) \quad [42]$$

$$u_2^{*\,1/2}/[DT_2^{*\,1/4}] = 0.36(r/H)^{-0.315} \quad [43]$$

$$dT_d/dt = u^{1/2}(T_g - T_d)/RTI \quad [45]$$

As previously mentioned, using these equations for the temperature and velocity of fire gases requires that the heat transfer equation be solved numerically. If it is assumed that dT_d/dt is constant over a short period of time, Dt (delta T), the following approximation can be made to determine the change in the detectors temperature at the end of that time increment.

$$DT_d = u(T_g - T_d)Dt/RTI \quad [45]$$

Here T_d is the temperature of the detector at the start of the time increment. DT_d is delta T, the change in detector temperature over the time interval Dt.

These equations will be used to solve two types of problems which a fire protection engineer might face. The first is to design a fire detection system that will provide a specified amount of escape time or respond when the fire reaches a certain threshold heat output. The second situation is one where an engineer must analyze the response time of a fire detection system or the size of the fire at detector response. The second problem type will be considered after the introduction of Beyler's equations.

In the first example the required response time of the

detector or the threshold size fire that the detector should respond to must be estimated. It is also necessary to estimate the rate at which the fire will grow. These are engineering judgments which must be made for each situation which is being studied. Examples provided later will assist in making these judgments.

With a given alpha or t_c, the response time t_r, and threshold fire size at response Q_T, are interchangeable through the power-law fire growth equation:

$$Q_T = at_r^2 \quad \text{or} \quad t_r = (Q_T/a)^{1/2} \qquad [46]$$

A detector type must be selected for analysis. For this discussion assume that the detector will be a fixed temperature heat detector or sprinkler. The operating temperature of the unit is T_s. The sensitivity of the unit is described by RTI or Γ_0.

The ambient temperature T_a, and the ceiling height H, of the area under consideration must also be estimated. If the minimum expected ambient temperature is used, answers will be conservative since the detector must absorb enough heat to go from ambient temperature to its operating temperature. The height above the fuel surface or the height above the virtual origin of the flame can be used in lieu of the ceiling height. When the larger of the possible choices

for H is used, answers are more conservative.

Based on the information above, the design problem is to determine how close this particular detector must be to the fire to respond in t_r seconds or when the heat output of the fire is Q_T BTU/sec or kW. This is the radial distance r, between the detector and the axis of the fire plume. For this set of conditions a first guess for r must be made. The equations are then solved for the fire size or response time of the detector.

If the fire size at response is larger than the size fire that must be detected, the detector must be moved closer to the fire. Similarly, if the response time is longer than the goal, a smaller r must be tried. On the other hand, if Q or t at detector response is smaller than the target values, a larger r is tried.

This iterative process continues until the fire size at detector response or time to detector response coincides with the established goals. The actual solution of this type of problem is outlined below.

1. Determine the environmental conditions of the area being considered.
   a. T_a
   b. H
2. Estimate the fire growth characteristic alpha or t_c

for the fuel expected to be burning.

3. Establish the goals of the system: t_r or Q_T.
4. Select the detector type to be used. For fixed temperature units this establishes the detector response temperature and its RTI or Γ_0.
5. Make a first estimate of the distance r from the fire to the detector.
6. Assume that the fire starts obeying the power-law model at time t = 0.
7. Set the initial temperature of the detector and its surroundings at ambient temperature.
8. Increment the temperature of the fire gases flowing past the detector by a small amount DT.
9. Calculate the corresponding change in the reduced gas temperature DT_2*, from Equation 39.
10. Calculate the corresponding reduced time t_2*, to reach this gas temp. using Equations 41 and 42.
11. Calculate the actual time using Equation 38.
12. Use the power-law fire growth equation to calculate the fire size which corresponds to the time calculated in step 11.
13. Calculate the reduced velocity of the fire gases flowing past the detector using Equation 43.
14. Equation 40 is used to calculate the actual velocity of the gases.
15. If Γ_0 and u_0 of the detector are known, use Equation 29 to calculate the corresponding RTI. If

the RTI is known, proceed to the next step.

16. Equation 44 can now be used to calculate the resulting temperature of the detector.

17. Repeat steps 8 through 16 until the detector reaches its operating temperature.

18. The time to detector response (or Q calculated with the response time) is now compared to the detector response goal established in step 4.

19. a. If the detector response was too slow or the fire size at response was too large, select a smaller value for r and repeat this procedure starting with step 6.

    b. If the detector response was faster than necessary or the fire size at response was smaller than needed, select a larger value for r and begin again with step 6.

Repeat this procedure until a detector position r, is converged upon. The distance r is the farthest that this particular detector can be located from the fire, if it is to respond within the goals established. On a ceiling where detectors are to be evenly spaced, the point which is farthest from any detector will be in the middle of four detectors. See Figure 17. The maximum spacing between detectors is:

$$S = 2^{1/2}r \qquad [47]$$

FIGURE 17

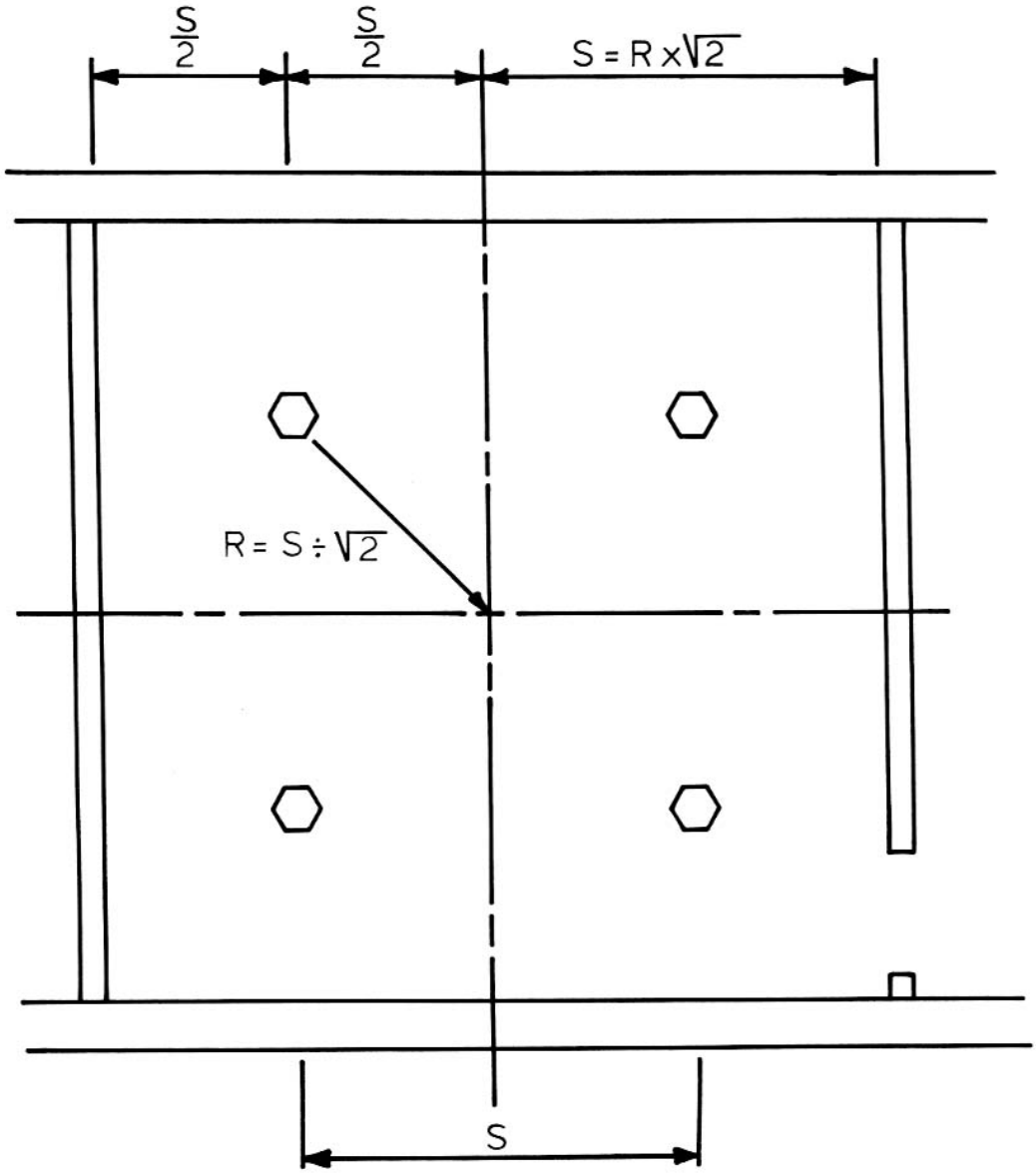

This same procedure can be used to determine the required spacing of different types of fire detectors. A detector with a lower operating temperature or one with a higher sensitivity could be installed at a greater spacing and still respond within the established system goals.

As mentioned earlier, the response of rate compensated and rate of rise heat detectors can not be modeled exactly using the concept of response time index. However a response time index could be used to estimate the response of these types of detectors. The limitation is that the RTI can only be expected to be precise when the fire gas temperatures and velocities are the same or close to those used in the plunge test used to determine the RTI. The technique outlined above could then be used to get an approximate required detector spacing. For rate compensated heat detectors, the procedure would be the same as outlined above for fixed temperature heat detectors.

For rate of rise heat detectors the procedure is exactly the same except in step 16, DT/Dt is calculated. The procedure is repeated until the rate of temperature rise is equal to the rate at which the detector will respond.

7. SMOKE DETECTOR RESPONSE MODEL

The relationship between optical density and the change in temperature along the ceiling for a given combustible, which Heskestad and Delichatsios proposed, can be used with the similarity equations to estimate the response of smoke detectors. This approximation is roughly independent of the operating principle of the detector. At the present time this approximation has not been independently verified and is presented here only for the purpose of discussion.

There are two basic types of commercially available smoke detectors. One type is an ionization smoke detector. In this type of detector there are two oppositely charged plates separated by an air space. Above the air space is a small radioactive element which ionizes the air between the two plates. The electrical potential between the plates causes the negatively charged air particles to flow towards the positively charged plate. The positively charged particles flow towards the negatively charged plate. When smoke enters the air space it attaches itself to the ions and reduces the current flow between the two plates. This change is detectable by the electronics of the detector.

Most photoelectric smoke detectors operate by sensing light which is scattered by smoke in the detector's chamber. A small light source (usually infrared light) projects a light beam in the chamber of the detector. When smoke enters

the chamber. some of the light is scattered off of the smoke and onto a light sensor. The detector activates when a specific amount of light is reflected onto the light sensor.

Based on the discussion above, it can be seen that ionization detectors are sensitive to the quantity and size of the smoke particles in the chamber of the detector. Photoelectric detectors are sensitive to the quantity and reflective properties of the smoke. For a given combustible material, Heskestad and Delichatsios assumed that the properties of the smoke (specifically particle size distribution and reflective properties) do not vary appreciably as it travels from the fire to the detector. This theory also assumes that transport of the smoke to the detector is by buoyant forces only.

It is then concluded that for a given detector (both operating principle and specific design) and material combination, response will occur when the change in fire gas temperature reaches a specific threshold level. This change in temperature at response has been called the Detector Material Response Number (DMR) [5].

Further test data must be generated and analyzed before this type of smoke detector model can be used as a definitive guide in determining the response of commercially available smoke detectors. If the theory is valid, it will be

necessary to determine DMR's for each commercially available smoke detector. It will also be necessary to determine the characteristic length of the detector which is a measure of the resistance smoke will experience in entering the detector chamber [6]. In an analogy to heat detectors, the DMR is similar to operating temperature and the characteristic length is analogous to tau or RTI. Once these detector characteristics are determined, the similarity equations would be used to calculate the change in temperature of the fire gases along the ceiling, and hence, the operation of the detector.

8. ANALYTICAL SOLUTION FOR DESIGNING SYSTEM RESPONSE

The solution of the equations presented requires thousands of mathematical operations which are best solved by a computer. Dr. Craig Beyler wrote a program which would solve the similarity equations and the heat transfer equation. That program was used by the NFPA 72-E Appendix C Subcommittee to generate a series of graphs and tables which engineers could use to determine the spacing of detectors required to detect specific fire scenarios.

As part of a graduate course titled "Computers in Fire Protection Engineering" at Worcester Polytechnic Institute, this author independently wrote a program which solved the same modeling problem. This program verified the results obtained by Dr. Beyler.

The main drawback to the solution of the equations presented here is that the heat transfer equation is solved numerically. The equations put forth by Heskestad and Delichatsios could not be substituted into the heat transfer equation and integrated to obtain an exact analytical solution.

In the original paper on the subject [20], Heskestad and Delichatsios presented the following equations which are slightly different than those presented in the report done for the Fire Detection Institute [6].

$$u_p^* = u/[A^{1/(3+p)} a^{1/(3+p)} H^{(p-1)/(3+p)}] = f(t_p^*, r/H) \quad [48]$$

$$DT_p^* = g(t_p^*, r/H)$$

$$= DT/[A^{2/(3+p)} (T_a/g) a^{2/(3+p)} H^{-(5-p)/(3+p)}] \quad [49]$$

where

$$t_p^* = t/[A^{-1/(3+p)} a^{-1/(3+p)} H^{4/(3+p)}] \quad [50]$$

$$A = g/(C_p T_a r_0) \quad [51]$$

The relationships presented in the FDI reports were simplified by dropping the terms containing A. Using these functional relationships Heskestad and Delichatsios presented the following correlations [20]:

$$t_{2f}^* = 0.954(1 + r/H) \quad [52]$$

$$DT_2^* = 0 \text{ for } t_2^* < t_{2f}^*$$

$$DT_2^* = \{[t_2^* - t_{2f}^*]/[0.188 + 0.313 r/H]\}^{4/3} \text{ for } t_2^* \geq t_{2f}^* \quad [53]$$

$$u_2^*/(DT_2^*)^{1/2} = 0.59(r/H)^{-0.63} \quad [54]$$

Beyler found that these correlations could be substituted into the heat transfer equation and integrated [21]. The analytical solution was published in his article in Fire Technology [7] and is repeated here.

$$T_d(t) - T_d(0) = (DT/DT_2^*) DT_2^* [1 - (1 - e^{-Y})/Y] \quad [55]$$

$$dT_d(t)/dt =$$

$$[(4/3)(DT/DT_2^*)(DT_2^*)^{1/4}(1 - e^{-Y})]/[(t/t_2^*)D] \quad [56]$$

where

$$Y = (3/4)(u/u_2^*)^{1/2} [u_2^*/(DT_2^*)^{1/2}] (DT_2^*/RTI)(t/t_2^*)D \quad [57]$$

$$D=0.188+0.313r/H \quad [58]$$

The solution of a design problem using these equations is similar to that described for the equations proposed by Heskestad and Delichatsios. The difference is that the heat transfer equation no longer has to be numerically integrated.

In a design situation, the objective is to determine the spacing of detectors required to respond to a specific fire scenario. The detector must respond when the fire reaches a certain threshold heat release rate or in a specified amount of time. Time and heat release rate are interchanged using the power-law fire growth model. The steps in solving this type of problem are as follows.

1. Determine the environmental conditions of the area being considered.
   a. T_a
   b. H
2. Estimate the fire growth characteristic alpha or t_c for the fuel which is expected to be burning.
3. Establish the goals of the system: t_r or Q_T.
4. Select the detector type to be used. For fixed temperature units this establishes the detector response temperature and its RTI or Γ_0.
5. Make a first estimate of the distance r, from the fire to the detector.

6. Assume that the fire starts obeying the power-law model at time t = 0.
7. Set the initial temperature of the detector and its surroundings at ambient temperature.
8. Using Equation 52, calculate the nondimensional time t_{2f}*, at which the initial heat front reaches the detector.
9. Calculate the factor A defined in Equation 51.
10. Use the required response time along with Equation 50 and p=2 to calculate the corresponding reduced time t_2*.
11. If t_2* is greater than t_{2f}*, continue with step 12. If not, try a new detector position r and return to step 8.
12. Calculate the ratio u/u_2* using Equation 48.
13. Calculate the ratio DT/DT_2* using Equation 49.
14. Use Equation 53 to calculate DT_2*.
15. Equation 54 is used to calculate the ratio $u_2^*/(DT_2^*)^{1/2}$.
16. Use Equations 58 and 57 to calculate Y.
17. Equation 55 can now be used to calculate the resulting temperature of the detector.
18. If the temperature of the detector is below its operating temperature, this procedure must be repeated using a smaller r. If the temperature of the detector exceeds its operating temperature, a larger r can be used.
19. Repeat this procedure until the detector

temperature is about equal to its operating temperature. The required spacing of detectors is then S=1.41r.

This same procedure is used to estimate the response of rate of rise heat detectors. The difference is that in step 17 Equation 56 is used to calculate rate of change of the detector temperature. This is then compared to the rate at which the detector is designed to respond.

Beyler's integration eliminates thousands of mathematical operations by eliminating the iterative solution to the heat transfer equation. It is still necessary, however, to converge on the correct detector spacing by iterating on the protection radius r. The use of a computer program is still required if this technique is to be a common tool for fire protection engineers.

Appendix B contains the listing of a computer program written to solve this particular set of equations. The program was written in FORTRAN and conforms to the ANSI X3.9-1978 subset requirements. Therefore, the program should be easily portable to systems using compilers which conform to this standard. The complete program includes comments inserted in the code for clarification.

9. ANALYTICAL SOLUTION FOR ANALYZING SYSTEM RESPONSE

Discussion so far has centered around the solution of a design problem. The question asked was: How far apart must detectors of a specific design be spaced, to respond within specific goals to a certain set of environmental conditions and a specific fire scenario?

The second type of problem which must be addressed is the analysis of an existing system or the analysis of a proposed design. Here the spacing of detectors or sprinklers is known. The engineer must still estimate the burning characteristics of the fuel and the environmental conditions of the space being analyzed. The equations can then be solved in a reverse fashion to determine the rate of heat release or the time to detector response. The technique is as follows.

1. Determine the environmental conditions of the area being considered.
   a. T_a
   b. H
2. Estimate the fire growth characteristic alpha or t_c for the fuel expected to be burning.
3. Determine the spacing of the existing detectors or sprinklers. The protection radius is then: $r=s/(2^{1/2})$.
4. Determine the detectors' rated response temperature

and its RTI or Γ_0.

5. Make a first estimate of the response time of the detector or the fire size at detector response. They are related through the power-law fire growth equation: $Q=at^2$.
6. Assume that the fire starts obeying the power-law model at time t = 0.
7. Set the initial temperature of the detector and its surroundings at ambient temperature.
8. Using Equation 52, calculate the nondimensional time t_{2f}*, at which the initial heat front reaches the detector.
9. Calculate the factor A defined in Equation 51.
10. Use the estimated response time along with Equation 50 and p=2 to calculate the corresponding reduced time t_2*.
11. If t_2* is greater than t_{2f}*, continue with step 12. If not, try a longer estimated response time and return to step 8.
12. Calculate the ratio u/u_2* using Equation 48.
13. Calculate the ratio DT/DT_2* using Equation 49.
14. Use Equation 53 to calculate DT_2*.
15. Equation 54 is used to calculate the ratio $u_2^*/(DT_2^*)^{1/2}$.
16. Use Equations 58 and 57 to calculate Y.
17. Equation 55 is now be used to calculate the resulting temperature of the detector.

18. If the temperature of the detector is below its operating temperature, this procedure is repeated using a larger estimated response time. If the temperature of the detector exceeds its operating temperature, a smaller response time is used.
19. Repeat this procedure until the detector temperature is about equal to its operating temperature.

As in the design problem, this technique can be used to estimate the response of existing systems of rate of rise heat detectors. The difference is that in step 4 the set point or rate of temperature rise at which the detector will respond, must be determined. In step 17 Equation 56 is used to determine the rate at which the temperature of the detector is changing.

The program listed in Appendix B includes the routines necessary to analyze existing systems or proposed designs.

To facilitate the use of this design and analysis technique, a second computer program was written. The second program generates design tables and analysis tables which can be used in lieu of a computer to solve problems. Appendix C contains this program. As with the first program, it was written in standard FORTRAN to insure portability to a wide range of machines with FORTRAN compilers.

Appendix D contains a set of tables, generated by the computer program, which can be used to design fixed temperature detection systems. A set of tables which can be used to analyze existing systems or proposed designs is contained in Appendix E. Interpolation between values contained in the tables is valid to obtain solutions to a wider range of problems. The tables were generated using English units (feet, degrees Fahrenheit and BTU's) and were rounded to the nearest whole number.

10.0 ERRORS RESULTING FROM THE USE OF A P = 2, POWER-LAW MODEL

When the exact history of velocity and temperature of fire gases flowing past a detector is not known, errors are introduced in the design and analysis of fire detector response. In their report, Heskestad and Delichatsios did not directly discuss the impact of errors resulting from the use their equations, as opposed to actual data, on the design or analysis of detector response. However, graphs in their report do show the errors in calculated fire gas temperatures and velocities [6]. An exact treatment of these errors is beyond the scope of this thesis, though some discussion is warranted. The purpose of this section is estimate the magnitude of errors resulting from the use of a p = 2, power-law fire growth model.

Plots of actual data and calculated data show that errors in DT_2* can be as much as 50%, though generally there appears to be much better agreement [6]. The maximum errors occur at r/H values of about 0.37. All other plots of actual and calculated data, for various r/H, show much smaller errors. In terms of the actual change in temperature over ambient, the maximum errors are on the order of 5 to 10 °C. The larger errors occur with faster fires and lower ceilings.

At r/H = 0.37, the errors are conservative when the equations are used in a design problem. That is, the

equations predicted lower temperatures. Plots of data for other values of r/H indicate that the equations predict slightly higher temperatures.

Errors in fire gas velocities are related to the errors in temperatures. The relationship is shown in equations 10 and 7. These equations show that the velocity of the fire gases is proportional to the square root of the change in temperature of the fire gases [6]. In terms of heat transfer to a detector, the detector's change in temperature is proportional to the change in gas temperature and the square root of the fire gas velocity. Hence, the expected errors bear the same relationships.

Based on the discussion above, errors in predicted temperatures and velocities of fire gases will be greatest for fast fires and low ceilings. Sample calculations simulating these conditions show errors in calculated detector spacings on the order of plus or minus one meter or less.

As shown earlier, the p = 2, power-law fire model is not always the best model for a fire's heat release rate. Errors caused by assuming this type of fire growth can be estimated by calculating the response of a detector to several different fire growth scenarios. To accomplish this, a model which gives velocity and temperature of a ceiling jet for

different heat release rate histories is needed.

In 1972, R.L. Alpert of Factory Mutual presented a paper entitled "Calculation of Response Time Of Ceiling Mounted Fire Detectors" at the May meeting of the National Fire Protection Association. That paper was later published in Fire Technology [22]. In the paper, Alpert presented a series of equations which can be used to calculate the temperature and velocity of fire gases in a ceiling jet for fires with a constant heat release rate.

Those equations can be used to model a growing fire by assuming the fire to be composed of a series of steady heat release rates. The problem with this type of quasi-steady modeling is that the temperature and velocity of the fire gases at a point away from the source is assumed to be related to the instantaneous heat release rate of the fire. This neglects the time required for transport of the fire gases from the source to the detector. Despite this shortcoming, the quasi-steady model for fire gas temperatures and velocities can be used to estimate the magnitude of the difference in temperatures and velocities resulting from different heat release rate histories. More importantly, the effects on the design and analysis of detector response can be estimated.

The National Bureau of Standards has published a computer program called DETACT-QS which uses Alpert's

equations to calculate the response of heat detectors [23]. That program requires the following input: ceiling height (H), ambient temperature (T_a), distance from fire axis to detector (r), detector activation temperature (T_s) and detector response time index (RTI). The user must also input a time versus heat release rate history for the fire.

Analyses using DETACT-QS were conducted using actual heat release rates, heat release rates predicted by a best fit model and heat release rates predicted by a p = 2 model, for NBS furniture calorimeter test numbers 22, 27, 31, 39, 56, 64 and 67. These heat release rates are shown graphically in Figures 6 through 13. To conduct the analyses, arbitrary values for H, T_a, r, T_s and RTI were selected. These data, as well as the results of the calculations, are summarized in Tables 6 through 13.

TABLE 6

Test Number 22

H = 3 m, r = 3 m, T_a = 10 °C, T_s = 57 °C, RTI = 50 $m^{1/2}sec^{1/2}$

Fire scenario.	Q_t kW	t_r sec
Actual test data:	645 kW	645 sec
p = 4.56, alpha = 8 x 10^{-11}:	560 kW	656 sec
p = 2, alpha = .0086 kW/sec^2, t_v = 400 sec:	605 kW	656 sec

TABLE 7

Test Number 27

H = 3 m, r = 6 m, T_a = 10 °C, T_s = 57 °C, RTI = 50 $m^{1/2}sec^{1/2}$

Fire scenario.	Q kW	t_r sec
Actual test data:	1874 kW	204 sec
p = 3.71, alpha = $5x10^{-6}kW/sec^2$:	1982 kW	207 sec
p = 2, alpha = .1055 kW/sec^2, t_v = 70 sec:	1925 kW	205 sec

TABLE 8

Test Number 31

H = 3 m, r = 6 m, T_a = 10 °C, T_s = 57 °C, RTI = 50 $m^{1/2}sec^{1/2}$

Fire scenario.	Q kW	t_r sec
Actual test data:	2251 kW	239 sec
p = 6.67, alpha = $4x10^{-13}kW/sec^2$:	2623 kW	238 sec
p = 2, alpha = .2931 kW/sec^2, t_v = 145 sec:	2536 kW	238 sec

TABLE 9

Test Number 39

H = 3 m, r = 6 m, T_a = 10 °C, T_s = 57 °C, RTI = 50 $m^{1/2}sec^{1/2}$

Fire scenario.	Q kW	t_r sec
Actual test data:	3092 kW	84 sec
p = 2.58, alpha = .0331 kW/sec^2:	3239 kW	86 sec
p = 2, alpha = .8612 kW/sec^2, t_v = 20 sec:	3548 kW	84 sec

TABLE 10

Test Number 56

H = 1 m, r = 1 m, T_a = 10 °C, T_s = 57 °C, RTI = 26 $m^{1/2}sec^{1/2}$

Fire scenario.	Q kW	t_r sec
Actual test data:	34 kW	122 sec
p = 1.16, alpha = .1553 kW/sec^2:	39 kW	118 sec
p = 2, alpha = .0042 kW/sec^2, t_v = 50 sec:	50 kW	159 sec

TABLE 11

Test Number 64

H = 3 m, r = 2 m, T_a = 10 °C, T_s = 57 °C, RTI = 50 $m^{1/2}sec^{1/2}$

Fire scenario.	Q kW	t_r sec
Actual test data:	360 kW	1289 sec
p = 3.79, alpha = $5x10^{-10}$ kW/sec^2	307 kW	1289 sec
p = 2, alpha = .0011 kW/sec^2, t_v = 750 sec:	318 kW	1288 sec

TABLE 12

Test Number 67, Initial growth.

H = 3 m, r = 2 m, T_a = 10 °C, T_s = 38 °C, RTI = 50 $m^{1/2}sec^{1/2}$

Fire scenario.	Q kW	t_r sec
Actual test data:	150 kW	490 sec
p = 1.96, alpha = .0008 kW/sec^2:	124 kW	445 sec
p = 2, alpha = .0009 kW/sec^2, t_v = 90 sec:	124 kW	461 sec

TABLE 13

Test Number 67, Later growth.

H = 3 m, r = 2 m, T_a = 10 °C, T_s = 74 °C, RTI = 50 $m^{1/2}sec^{1/2}$

Fire scenario.	Q kW	t_r sec
Actual test data:	381 kW	690 sec
p = 3.19, alpha = $5x10^{-7}$ kW/sec^2:	565 kW	689 sec
p = 2, alpha = .0086 kW/sec^2, t_v = 400 sec:	648 kW	674 sec

The quasi-steady calculations show that maximum errors occur when modeling fires with low heat release rates such as Test 56 and with fires that do not grow steadily, such as Test 67. When all of the examples are considered, the errors in fire size at response for the p = 2 model versus the actual test data range from -17% to +70%. The magnitude of the average error was on the order of 23%. If Tests 56 and 67 are ignored, the errors fall into the range -12% to +15% with an average of plus or minus 10%.

In terms of the calculated response times, errors were in the range of -6% to +30% for the eight examples. The magnitude of the average error was on the order of 5%. Not including Tests 56 and 67, the errors ranged -0.4% to +1.7%. The magnitude of the average error in response time was then on the order of 0.6%.

These examples show that the p = 2, power-law fire growth model can be used to model a wide range of fire

scenarios. In general, errors in fire size at response will be on the order of plus or minus 10% to 15%. Errors in response time will be on the order of plus or minus 2%. Errors can be expected to be higher when the fire does not grow steadily or when heat releases are low (below about 200 kW).

When designing detection systems, errors in fire size and response time have an effect on the required detector spacing. In the example using Test 22, a change of plus or minus 15% in the fire size at detection results in a variation on required detector spacing of plus or minus 15%. In terms of actual spacing the range is from 5.8 m to 7.5 m. Similar calculations for the other examples show the errors in spacing to be of the same magnitude.

These estimates show that while curve fitting techniques can be used to more accurately model fire growth, good engineering judgment produces answers which are within acceptable limits. After all, in most design and analysis situations, the engineer must still make estimates of such factors as ceiling clearance and ambient temperature as well as the expected fuel and fuel geometry.

11. SELECTING PARAMETERS FOR DESIGN AND ANALYSIS

Someday, fire loads may be used by the fire community in the same way that structural engineers use earthquake zone maps to design for potential earthquakes. Electrical engineers might compare fire loads to fault currents used in designing overcurrent protection devices. For fire detection systems these loads can be called threshold limits at which detection must occur. Quantitatively, these limits can be expressed in terms of the maximum allowable fire size at response or the maximum response time of a system. At the present time, these requirements are not established by any building codes. It is the job of the design engineer to work with the building owner and local code officials to establish the system's performance requirements.

The threshold fire size used for designing a fire detection system will vary depending on the system's goals. Ultimately, the goals of the system can be put in three basic categories: life safety, property protection and business protection.

When designing for life safety, it is necessary to provide early warning of a fire condition. The fire detection and alarm system must provide a warning early enough to allow complete evacuation of the danger zone before conditions become untenable.

Property protection goals are principally economic. The objective is to limit damage to the building structure and contents. The maximum allowable losses are set by the building owner or risk manager. The goals of the system are to detect a fire soon enough to allow manual or automatic extinguishment before the fire exceeds the acceptable damage levels.

Goals for the protection of a mission or business are determined in a manner similar to that used in property protection. Here, fire damages are limited to prevent undesirable effects on the business or mission. Some items which need to be considered are the effects of loss of raw or finished goods, loss of key operations and processes and the loss of business to competitors during downtime.

Whether the prime concern is life safety, property or business protection, in order to use the response model presented in this paper, the system's goals must be translated to a required response time or a maximum allowable fire size. Establishment of a system's performance requires detailed study of many factors by the design engineer and a further discussion of this important step is beyond the scope of this thesis.

Once the goals of a system have been established the next step is to establish a worst case or most probable fire

scenario. This requires that the occupancy of the building and the expected fuels be analyzed to establish an expected fire growth rate (alpha, based on a p = 2, fire growth model) and an expected maximum heat release rate. Furniture calorimeter tests and other fire test data can be used to help estimate these parameters. It is important that the person doing the design or analysis test different fire scenarios to establish how the system design or response might change.

The vertical distance from the fire to the detector also has an effect on the design of a system. If known, the vertical distance from the fuel surface to the detector can be used. For a worst case design, the floor to ceiling height should be used.

As previously discussed, ambient temperature will effect the response of fixed temperature detectors and sprinklers. By using the lowest expected ambient temperature, designs and analyses will be conservative since detectors will have to absorb more heat to reach their operating temperature.

The computer program listed in Appendix B requires that a detector type (fixed temperature, rate of rise or smoke detector) be selected. In this sense the design process is trial and error. A particular detector's characteristics are entered and a required spacing is calculated. Different detector types and characteristics can be tried before a

final design is reached.

The range of input parameters selected can have varying effects on the outcome of design or analysis calculations. When doing a design or an analysis, these effects should be studied by systematically varying the input parameters over their expected range. This will show the sensitivity of a system to changes in variables which effect its performance.

12. DESIGN AND ANALYSIS EXAMPLES

Analysis and design problems will be used to show how fire protection engineers can use the techniques presented in this paper. The examples will also show the sensitivity of the system to changes in variables and input parameters. The problems were solved using the computer program contained in Appendix B. The tables contained in Appendix D and Appendix E could have been used in lieu of the computer program.

Example 1.

A warehouse is used to store sofas and other furniture. The sofas are similar to one tested by the National Bureau of Standards in their furniture calorimeter. Burning characteristics are assumed to be similar to the sofa used in Test 38 (see Appendix A): alpha = 0.1055 kW/sec^2 (t_c = 100 sec), peak heat release rate = 3000 kW. The sofas are stored one or two high.

The building itself has a flat roof and ceiling. The distance from the floor to the ceiling is 4.6 m (15 ft). When the sofas are stacked two high the distance from the top of the fuel package to the ceiling is 2.4 m (8 ft). Ambient temperature in the warehouse is kept above 10 °C (50 °F).

Based on maximum allowable property loss goals established by the owner, it is desirable to detect a fire

and notify the fire department prior to a second fuel package becoming involved. The original NBS report [12] contains data on radiation measured during Test 38. This information can be used along with techniques presented by Drysdale [15] to determine when a second item might ignite. For this example it is assumed that the fire must be detected when it reaches a heat release rate of about 527 kW (500 BTU/sec).

The fire detection system will consist of fixed temperature heat detectors connected to a control panel which is in turn is connected to the local fire department. The detector to be used will have a fixed temperature rating of 57 °C (135 °F) and an RTI of 42 $m^{1/2}sec^{1/2}$ (77 $ft^{1/2}sec^{1/2}$).

The problem is to determine the spacing of detectors required to detect this fire. When the computer program runs, the user is prompted for all of the above information. In this example the data is fixed except for the distance from the ceiling to the flame origin. If the distance between the top of the fuel and the ceiling (2.4 m) is used the program calculates that the detectors must be spaced 2.8 m (9.2 ft) apart to respond when the fire reaches a heat output of 527 kW (500 BTU/sec).

Equation 2 can be used to estimate the location of the fires virtual origin. Using an effective burning fuel diameter of 1.2 m the location of the virtual origin z_0, is

calculated to be -0.2 m. This indicates that the flame source is located 0.2 m below the top of the fuel surface. The distance to the ceiling is then 2.6 m. The calculated detector spacing is then found to be 2.6 m (8.5 ft).

For a worst case analysis, the distance from the floor to the ceiling (4.6 m) is used. This results in a required detector spacing of 1.2 m (3.9 ft). This results in an r/H ratio of 0.18. Because the correlations presented by Heskestad and Delichatsios are valid only for r/H greater than 0.37, the use of an installed spacing less than 2.6 m can not be justified by the calculations.

A more realistic worst case scenario would be when the sofas are not stacked two high. With one sofa on the floor the distance from the fuel to the ceiling would be about 3.7 m (12 ft). The required detector spacing would then be 1.8 m (5.9 ft). Again, this results in an r/H ratio less than 0.4. The smallest spacing which could be justified by the calculations is 1.5 m.

Example 2.

This example will show how to select a detector type to economically meet the system's goals. The fire scenario and goals used in Example 1 will be used with H = 2.4 m (8 ft).

In Example 1 it was found that heat detectors with a

fixed temperature rating of 57 °C (135 °F) and an RTI of 42 $m^{1/2}sec^{1/2}$ must be spaced 2.8 m (9.2 ft) apart to meet the system's goals. Here, the spacing of rate of rise heat detectors will be estimated.

The detector to be used is rated to respond when its temperature increases at a rate of 11 °C/min (20 °F/min) or more. The detector's RTI will be assumed to be the same as the detector in Example 1. The required spacing is calculated to be 7.1 m (23 ft).

If the total area of the warehouse is 2500 m^2, approximately 320 fixed temperature heat detectors would be required to meet the established goals. The same goals can be met with only 50 rate of rise heat detectors. Additional detectors might be required because of obstructing beams or walls.

Example 3.

In this example the effects of varying fire growth rate will be examined. The scenario used in the last example will be used again.

In Examples 1 and 2 the rate of fire growth was described by the power-law equation with an alpha of 0.1055 kW/sec (0.1000 BTU/sec^3) or t_c = 100 sec. If the fire were

to grow at a faster rate, a smaller spacing will be required to meet the system's goals. For instance, if t_c = 50 sec (a = 0.4220 kW/sec^2) the required spacing would be 1.5 m (4.9 ft). If t_c = 200 sec (a = 0.0264 kW/sec^2) the spacing is increased to 3.9 m (12.8 ft).

Example 4.

This example shows how existing systems or proposed designs are analyzed. Again the scenario used in the previous examples will be assumed. The height of the ceiling above the fire is 2.4 m (8 ft). The detectors are 570C (135 °F) fixed temperature heat detectors spaced 2.8 m (9.2 ft) on center. The detector has an RTI of 42 $m^{1/2}sec^{1/2}$ (77 $ft^{1/2}sec^{1/2}$). Ambient temperature is 10 °C (50 °F).

The detection system being analyzed is designed to respond to a 527 kW (500 BTU/sec) which is growing according to $Q = at^2$, with a = 0.1055 kW/sec^2. What would happen if there was an occupancy change and the new fuel loading had different burning characteristics than the fuel which the system was designed for? If the fuel burns faster or slower, what will be the fire size when the detector responds?

Using the program in Appendix B several different fire growth rates were tried. If t_c = 50 seconds the system will respond when the fire reaches a heat output of about 886 kW. If t_c = 150 seconds, Q_T = 413 kW. Table 14 shows the results

of calculations for other values of t_c.

Table 14 shows that at faster fire growth rates the detector responds sooner, but the fire size at response is larger. At slower growth rates the detector responds when the fire is much smaller. At the faster rates, ceiling temperatures quickly exceed the response temperature of the detectors. However, the inherent thermal lag of the detector delays response until the detector absorbs enough heat to reach its operating temperature.

TABLE 14

Problem 4. Fire growth rate versus fire size at response.

t_c (sec)	alpha (kW/sec^2)	Q_T (kW)	t_r (sec)
50	0.422	886	46
75	0.1876	670	60
100	0.1055	527	71
150	0.0469	413	94
200	0.0264	347	115
500	0.0042	221	229
1000	0.0011	177	409

When the fire grows at slow rates, detector temperatures are closer to the actual fire gas temperatures. The thermal

lag of the detector is not as significant as the fire's ability to increase the ceiling jet gas temperatures.

Example 5.

A sprinkler system is being installed in a large exhibition hall. The building has a flat roof deck supported by open space frame trusses. The distance from the underside of the roof deck to the floor is 12 m (39.3 ft). Ambient temperatures do not usually fall below 5 °C (41 °F).

Three different designs for the sprinkler system have been proposed. All three are designed to provide the same water density over a specified area. Each proposal uses a sprinkler with a temperature rating of 74 °C (165 °F) and an RTI of 110 $m^{1/2}sec^{1/2}$ (200 $ft^{1/2}sec^{1/2}$). The only difference between the three systems is the spacing of the-sprinklers and the branch lines that feed them. The first proposal uses a square array with a spacing of 3 m (10 ft). The second and third proposals are based on square array spacings of 3.7 m (12 ft) and 4.6 m (15 ft) respectively.

What effect will the three different spacings have on the size of the fire when the system responds? Assume two different fire scenarios. In the first the fire grows at a moderate rate with t_c = 200 seconds. The second fire scenario has a slower fire growth rate with t_c = 500 seconds.

The computer program in Appendix B was used to solve the problem. Results of the calculations are shown in Table 15.

Table 15 shows an increase of about 25 % in the fire size at response when the spacing is increased 50 % from 10 m to 15 m. The increased spacing may result in a lower system cost. However, closer spacings mean that the sprinkler system will probably respond sooner. The fire protection engineer can use this type of analysis to assist in choosing a system which best meets the project's overall goals.

TABLE 15

Example 5. Effect of spacing on fire size at response.

	t_c=200 seconds		t_c=500 seconds	
S (m) meters	Q_T kW	t_R min	Q_T kW	t_R min
10	5128	7.3	4340	16.9
12	5660	7.7	4788	17.8
15	6398	8.2	5415	18.9

Example 6.

Example 6 illustrates the effect of temperature difference on the response time of fixed temperature detector and sprinkler actuation. It is the change in temperature,

the difference between its operating temperature and the ambient temperature, which effects response time.

When selecting fixed temperature heat detectors and automatic sprinklers it is desirable to select a temperature rating that is as close as possible to the expected maximum ambient temperature. This reduces the response time of the detector in a fire condition. The closer the response temperature is to ambient temperature, the less heat the detector must absorb to respond.

If the operating temperature of the detector is too close to ambient temperatures, false detector actuations can occur. NFPA 72-E [l] recommends a detector rating of 25 °F (14 °C) above the expected maximum ambient temperature.

The fire scenario used in Example 5 will be used to quantify the effects of temperature difference on response time and fire size at response. The question asked is: What effect would the use of sprinkler heads with different temperature ratings have on the response time and the size of the fire at response?

Calculations are done for a sprinkler head spacing of 3 m (10 ft). Sprinkler heads having temperature ratings of 57, 74, 93 and 100 °C (135, 165, 200 and 212 °F) are analyzed. The results of the computer calculations are shown in Table 16.

TABLE 16

Example 6. Effect of temperature difference on response.

			tc=200 seconds		tc=500 seconds	
T_s °C	T_a °C	DT_d °C	Q_T kW	t_r min	Q_T kW	t_r min
57	5	52	3654	6.2	2972	14.0
74	5	69	5128	7.3	4340	16.9
93	5	Be	6952	8.6	6057	20.0
100	5	95	7668	9.0	6736	21.1

Table 16 shows that there is a large difference in fire size at response when high temperature heads are used in lieu of the lower temperature heads. If this were a detection system the lower temperature units would be the obvious choice.

With a sprinkler system other factors such as the number heads opening must be considered. While the lower temperature rating means quicker response, it also means that more heads may open. However, quicker response might mean that the sprinkler system can control or extinguish the fire before additional heads open. These factors must also be considered by the design engineer.

13. DISCUSSION

Examples 1 through 6 show how the material presented in this thesis is used to design and analyze the response of fire detection systems and automatic sprinkler systems.

Example 1 shows how the computer program contained in Appendix B is used to design detection systems to meet specific goals. The example also shows the effects of ceiling height on a design.

The greater the distance from the fire to the ceiling, the closer the detectors must be spaced to respond within the goals of the system. Designs based on the floor to ceiling distance are conservative and representative of a worst case condition. A more realistic design might be based on the most probable or the greatest expected ceiling clearance.

A method to perform cost-benefit analyses of proposed designs is presented in Example 2. By trying different detector types or detectors with higher sensitivities, project goals might be met with a fewer number of detectors.

The scenario in Example 2 shows that to detect the same fire, a much greater number of fixed temperature heat detectors is required, than of rate of rise heat detectors. This is not always the case. Many fires will develop slowly and cause high ceiling temperatures without ever exceeding

the rate of temperature rise necessary to actuate a rate of rise heat detector. As a back-up, most commercially available rate of rise heat detectors have a fixed temperature element also. Of course the rate of rise element and the fixed temperature element should be considered separately when designing or analyzing a system.

The effect of fire growth rate on detector response is illustrated in Examples 3 and 4. Example 3 shows that for new designs, detector spacing must be greatly reduced to detect a rapidly developing fire. Similarly, slowly developing fires can be detected with fewer detectors, installed at larger spacings. Example 4 shows that for a given installation, the rate of fire growth has an effect on the size fire at response. With more rapidly growing fires, larger heat release rates will be reached before detector activation than with slowly developing fires.

Table 14 is a summary of Example 4. It clearly shows that changes in fuels or the burning characteristics of a fuel will alter the response of the system. This type of analysis illustrates the importance of designing a system for its expected occupancy. As the use of the building changes so will the characteristics of the fuels in the building. Analyses such as this can be conducted to determine if the system requires any modifications to continue meeting its goals.

Examples 5 and 6 show how the design and analysis techniques presented in this paper should be incorporated in all phases of a buildings fire protection design. These techniques can be used to show that designs which might appear to be equal, really are not. This provides the fire protection engineer with a way to measure the effectiveness of detection systems and provides a quantitative scale which can be used to compare various system designs.

14. CONCLUSIONS

The power-law fire growth model $Q = at^2$, was tested against heat release rate data from independent tests done at the National Bureau of Standards [12][16]. The NBS data used to test the model came from furniture calorimeter tests. There is generally good correlations between test data and the model even when the parameters for the p = 2 model were not determined by regression analysis. This indicates that the power-law equation can be used to model the heat release rates of open air furniture fires.

Equations were presented to calculate fire gas temperatures and velocities. The equations were proposed by Heskestad and Delichatsios [6] to model temperatures and velocities along a flat ceiling with no walls. The equations are for fires which follow the p = 2, power-law fire growth model.

Response models for fixed temperature heat detectors and sprinklers, rate of rise heat detectors and smoke detectors were presented and discussed. Fixed temperature models are considered to be the most accurate. There is less confidence in the models presented for rate of rise heat detectors and smoke detectors. Additional research is needed to develop and test response models for these detector operating principles.

The response models presented are for flaming fires only. They do not model smoldering combustion. Research on the production and movement of fire signatures during smoldering combustion is needed. There has already been some work in the area of smoke production [15] but not much in the area of transport.

The response models combined with the fire model equations presented by Heskestad and Delichatsios require numerical techniques to affect a solution. The solution was outlined and discussed in detail.

A set of modified equations proposed by Heskestad and Delichatsios and solved analytically by Beyler [7] were presented. The analytical solution was described in detail. The solution of the equations for both design and analysis problems was outlined.

Potential sources of errors in design and analysis problems were discussed. The material presented shows that there is higher confidence when the expected fire grows steadily and peaks above approximately 200 kW. Then errors in calculated spacings or fire size at response are on the order of 10% to 15%. Examples show how the engineer can vary input parameters to estimate the sensitivity of a system design to potential errors or changes in the parameters.

Computer programs were written to solve the fire growth model and the detector response model. The first program allows fire protection engineers to design or analyze the response of fire detection systems or automatic sprinkler systems.

A second computer program was written to generate tables which could be used to design or analyze fire detection or sprinkler systems. This program was used to generate the tables in Appendix D and Appendix E.

Examples presented demonstrate the use of the material presented in this thesis. The examples clearly show how new systems can be designed to meet specific objectives. Examples were also presented to show how existing systems or proposed designs can be analyzed.

The methods outlined in this thesis are tools which fire protection engineers can begin using immediately. These methods allow the response of detection and suppression systems to be engineered. This means that systems can now be designed and installed with greater confidence in their ability to perform as needed or intended.

The techniques presented allow system response to be quantified. However, a great deal of engineering judgment is still required in the design and analysis of the systems. Hence, the solutions are only as good as the data which the

engineer uses to generate them. The methods are best used to estimate the effects of changes in design or analysis parameters on a system's response rather than to try and accurately predict system response to a single set of variables.

This thesis also identifies areas where additional research or information is needed. Manufacturers of heat detectors and the agencies which test them must begin publishing information on the RTI of the units. Better models for the response of rate anticipation and rate of rise heat detectors must be developed. More research is needed to develop response models for smoke detectors. Finally, there is a great need for more research an modeling the production and transport of smoke and toxic gases during smoldering combustion.

References

1. "NFPA 72E Standard an Automatic Fire Detectors", National Fire Protection Association, Batterymarch Park, Quincy, MA 02269.

2. "NFPA 13 Standard on the Installation of Sprinkler Systems", National Fire Protection Association, Batterymarch Park, Quincy, MA 02269.

3. "Loss Prevention Data", Factory Mutual Engineering Corp., Norwood, MA 02062.

4. "Recommended Practices", Industrial Risk Insurers, Hartford, CT 06102.

5. I. Benjamin, G. Heskestad, R. Bright and T. Hayes, "An Analysis of the Report on Environments of Fire Detectors", Fire Detection Institute, 1979.

6. G. Heskestad and M. Delichatsios, "Environments of Fire Detectors - Phase I: Effect of Fire Size, Ceiling Height and Material." Volume I "Measurements" (NBS-GCR-77-86), May 1977, Volume II “Analysis" (NBS-GCR-77-95), June 1977, National Technical Information Service (NTIS) Springfield, VA 22151.

7. C. Beyler, "A Design Method For Flaming Fire Detection", Fire Technology, Volume 20, Number 4, November, 1984.

8. G. Heskestad, "Similarity Relations for The Initial Convective Flow Generated by Fire", ASME Paper No. 72-WA/HY-17, 1972.

9. G. Heskestad, "Physical Modeling of Fire", Journal of Fire and Flammability, Volume 6, July 1975.

10. G. Heskestad, "Engineering Relations for Fire Plumes", Technology Report 82-8 Society of Fire Protection Engineers, 60 Batterymarch St., Boston, MA 02110, 1982.

11. J.D. Seader and W.P. Chien, "Physical Aspects of Smoke Development in an NBS Smoke Density Chamber," Journal of Fire and Flammability, Volume 6, July 1975.

12. V. Babrauskas, J.R. Lawson, W.D. Walton and W.H. Twilley, "Upholstered Furniture Heat Release Rates Measured with a Furniture Calorimeter", U.S. Department of Commerce, National Bureau of Standards, National Engineering Laboratory, Center for Applied Mathematics, Center for Research, Washington, D.C. Number NBSIR 822604, December 1982.

13. C. Huggett, "Estimation of Rate of Heat Release By Means of Oxygen Consumption Measurements", Fire and Materials. 4, 61-5, 1980.

14. W.J. Parker, "Calculation of the Heat Release Rate by Oxygen Consumption for Various Applications", U.S. Department of Commerce, National Bureau of Standards, National Engineering Laboratory, Center for Applied Mathematics, Center for Research, Washington, D.C. Number NBSIR 81-2427, 1982.

15. D. Drysdale, "An Introduction to Fire Dynamics", John Wiley and Sons, N.Y., N.Y., 1985.

16. J.R. Lawson, W.D. Walton and W.H. Twilley, "Fire Performance of Furnishings as Measured in the NBS Furniture Calorimeter, Part I", U.S. Department of Commerce, National Bureau of Standards, National Engineering Laboratory, Center for Applied Mathematics, Center for Research, Washington, D.C. Number NBSIR 83-2787, August 1993.

17. G. Heskestad and H. Smith, "Investigation of a New Sprinkler Sensitivity Approval Test: The Plunge Test," FMRC Serial Number 22485, Factory Mutual Research Corp., 1976.

18. J.P. Hollman, "Heat Transfer," McGraw-Hill Book Company, N. Y. , N. Y. , 1976.

19. W. Bissell, private communication.

20. G. Heskestad and M. Delichatsios, "The Initial Convective Flow in Fire," Seventeenth Symposium (International) on Combustion, The Combustion Institute, 1979.

21. C. Beyler, private communication.

22. R. Alpert, "Calculation of Response Time of Ceiling Mounted Fire Detectors," Fire Technology, Volume 8, 1972.

23. D. Evans and D. Stroup, "Methods to Calculate the Response Time of Heat and Smoke Detectors Installed Below Large Unobstructed Ceilings," U.S. Department of Commerce, National Bureau of Standards, National Engineering Laboratory, Gathersburg, MD. Number NBSIR 85-3167, February 1985, issued July 1985.